Strategy for including physical processes in the ECMWF variational data assimilation system

Jean-François Mahfouf * Roberto Buizza Ronald M. Errico †

European Centre for Medium Range Weather Forecasts
Shinfield Park, Reading (UK)

Abstract

This paper describes the strategy developed at ECMWF for including physical parametrizations in the tangent-linear and adjoint versions of the operational forecast model (IFS). A first set of sub-grid scale processes is defined for linearization purposes. It includes vertical diffusion, large scale condensation, gravity wave drag, moist convection and radiation. Some simplifications have been necessary with respect to the operational physics. The validity range of the tangent-linear approximation is examined and preliminary results of singular vector computations with physical processes are described. In future developments current linearized versions of moist convection and radiation will be improved. The impact of including physics in 4D-Var assimilation will be assessed and the adjoint of the physics will be used for the assimilation of satellite precipitation data.

1 Introduction

Linearized versions of Numerical Weather Prediction (NWP) models have recently been developed to solve problems of data assimilation (Talagrand and Courtier, 1987), sensitivity analysis (Rabier et al., 1996), instability analysis (Buizza and Palmer, 1995), and Kalman filtering (Bouttier, 1993). The central part of a variational data assimilation system is the minimization of a cost-function measuring the departure between model variables and corresponding information (observations, previous forecast). Given the dimension of the state variable of a global NWP model (10^6 for the ECWMF T213L31), the gradient of the cost-function with respect to the initial state can only be computed efficiently using an adjoint version of the NWP model. In instability studies, linear forward and adjoint versions of a forecast model are needed to compute perturbations with the fastest growth over finite time intervals. At ECMWF, these type of perturbations, named singular vectors, are used to construct the perturbed initial conditions of the Ensemble Prediction System (Molteni et al., 1996).

So far, the adjoint of the IFS (Integrated Forecasting System) model developed at ECMWF in collaboration with Météo-France (Courtier et al., 1991) does not include physical processes

*email : paf@ecmwf.int
†Present affiliation: N.C.A.R., P O Box 3000 Boulder, CO 80307 (USA)

apart from a simple vertical diffusion and surface drag scheme acting as a momentum sink (Buizza, 1994). The lack of physical processes is not too detrimental at mid-latitudes where most of the evolution of the flow can be interpreted in terms of dynamical instabilities, but the use of an adiabatic linear model is certainly less valid in tropical regions.

However, the inclusion of physical parametrizations in adjoint models is not straightforward. Physical processes are characterized by strong non-linearities like the transition from unstable to stable regimes in the planetary boundary layer, and on/off switches (e.g. deep convection takes place when moisture convergence is positive together with low level vertical instability). This means that the range of validity of the tangent-linear approximation is reduced when physical parametrizations are included in linear forward/adjoint models. In data assimilation, for example, this can cause convergence problems for the minimization algorithm (wrong estimate of the gradient of the cost-function, existence of multiple minima).

Very few studies have been undertaken to include physical parametrizations in linearized NWP models. However, preliminary results are encouraging. In data assimilation, depending on the model and the physical parametrizations involved, convergence can be obtained either without a particular treatment of the thresholds or with some regularization (Zou et al., 1993 ; Zupanski, 1993; Zupanski and Mesinger, 1995). In instability studies, Ehrendorfer et al. (1996) have shown that the inclusion of moist processes in the computation of singular vectors of a limited area model leads to faster growth, and to an increased number of phase-space directions along which perturbations may grow.

The main purpose of this paper is to describe the strategy adopted at ECMWF in order to progressively include physical processes within the tangent-linear and adjoint versions of the operational forecast model. In section 2, the need for including physical processes in the context of variational assimilation and singular vectors is explained, as well as expected improvements and problems. Section 3 describes a first set of linearized physical parametrizations ; the linearity of various physical processes is also examined. Preliminary results of singular vector computations with physical processes are presented in section 4. The last section considers future developments.

2 Importance of physical processes in linearized models

An adiabatic adjoint version of the IFS has been used for preliminary computations of singular vectors with a primitive equations model by Buizza (1993). He showed that the inclusion of physical processes is essential to get realistic initial perturbations. Indeed, without surface drag and vertical diffusion, large amplification rates are captured close from the surface in the linear model. However, these singular vectors are non meteorological because they cannot grow in the

full diabatic model where turbulent processes are effective. Rabier et al. (1993) performed a 4D-Var assimilation for the October 87' Storm over France and England. They showed that, for this explosive cyclogenesis, the lack of condensation in the model prevents realistic forecasts of the humidity field. Beside these two examples, it is well-known that in mid-latitudes, the validity of the geostrophic approximation allows the definition of dynamical constraints to produce consistent analysis of mass and wind fields (balance equation, projection of the flow on slow Rossby modes). Indeed, the energy source of mid-latitude circulations is mainly derived from the baroclinicity represented by large meridional temperature gradients. These constraints are no longer valid in the tropics where the circulations are basically diabatically driven (cooling by radiation and heating by moist convection principally). The lack of physical constraints on dynamical fields (mostly the divergent part of the flow) and on thermo-dynamical variables (temperature and moisture) is evidenced in data assimilation systems by the so-called spin-up problem. The hydrological cycle (precipitation, evaporation, clouds) is generally not in equilibrium with the model at initial time. Therefore, during the first hours of the forecast, evaporation and precipitation increase or decrease in order to achieve a quasi-balance.

The moisture analysis problem in the tropics is demonstrated in recent 4D-Var experiments performed by Rabier et al. (1997). These experiments indicate that the forecast scores are improved with respect to the current operational 3D-Var over both hemispheres at all ranges. However, scores in the tropics reveal an opposite behaviour. The lack of physical processes (particularly moist convection) in the tangent-linear and adjoint versions of the ECMWF model contributes, at least partially, to explaining the worse performance. A sensitivity study showed that, when reducing the vertical velocity $\dot{\eta}$ in the tropical belt, the zonal mean increments of specific humidity are smaller and the subsequent forecasts experienced less spin-down (Rabier et al., 1997).

Future satellite systems, like TRMM (Tropical Rainfall Measuring Mission) to be launched at the end of 1997, will provide high resolution measurements of radiances in channels sensitive to precipitable water and rainfall rates over sparse data areas like the tropical oceans (Simpson et al., 1996). But these new observations will only be useful for data assimilation if they can be compared with model counterparts given by sub-grid scale processes. In other words, the observation operators providing the link between these new data and model variables are the physical parametrizations. Surface precipitation data provide information on the vertically integrated latent heating profiles. They could be very useful for improving initial temperature and moisture fields in NWP models, particularly in the tropics (few radiosondes, importance of diabating heating). Various attempts have been made in that direction. They have been initiated by Krishnamurti et al. (1984) and are often refered to as *physical initialization* or *diabatic initialization*. So far, physical initialization is not extensively used in operational data assimilation

systems for two reasons. Physical initialization is built on empirical statistical relations between satellite radiances and rainfall rates, and empirical 'inversion techniques' are used to modify the model profiles of temperature and moisture to better match the 'observed' rainfall rates (Puri and Miller, 1990 ; Heckley et al., 1990 ; Kasahara et al., 1996). However with new radiometers and more efficient inversion techniques, physical initialization can be improved. More reliable remotely-sensed observations will be provided by the TRMM Microwave Imager (TMI) and variational techniques allow for a better comparison between satellite observed radiances and model variables. Recent encouraging results with synthetic observations of precipitation have been obtained by Fillion and Errico (1997) in a 1D-Var assimilation and by Tsuyuki (1996) in a 4D-Var assimilation.

Problems associated with the convergence of the minimization algorithm have been pointed out by Verlinde and Cotton (1993). A 4D-Var incremental approach has been devised by Courtier et al. (1994) to reduce the problems of non-linearities induced by the physics (another justification is a significant reduction of the computational cost). The trajectory is computed with the full non-linear model (high resolution, comprehensive physics), and a simplified linear model (low resolution, simplified physics) is used for solving the minimization problem in the vicinity of the trajectory. Assimilation experiments of SSM/I precipitable water, performed by Filiberti et al. (1997), have shown improvements of the incremental formulation on the analysis of humidity for the October 87 severe storm situation with respect to Rabier et al.'s (1993) results. A consequence of 4D-Var incremental is that a progressive inclusion of physical processes in the linearized versions of the model will not increase the non-linearity of the problem. The cost-function to be minimized corresponds to the full model with comprehensive physics. The minimization problem solved in terms of increments will remain quadratic when including linearized physics. Therefore, physical processes will not increase convergence problems in the minimization algorithm with a 4D-Var incremental approach, although a positive impact on the quality of analyses remains to be proved.

3 The ECMWF linearized physics

3.1 General strategy

Results summarized in the previous section have clearly shown the importance of including vertical diffusion and moist processes in the tangent-linear (TL) and adjoint (AD) versions of the IFS model.

As a consequence, a first set of linearized physics has been devised for use in the TL/AD versions of the IFS. For a number of reasons explained hereafter, this physical package contains simplifications and modifications with respect to the operational one. The dominant physical

processes (and interactions) given the time scale of interest (1 day) have been linearized, but some of them are highly simplified. It is believed that the most important feedback mechanisms between the processes are nevertheless described.

The strategy adopted is to remain as close as possible to the operational package of physical parametrizations. This choice avoids the need for validating the parametrizations in the non-linear model. For example, we have chosen to keep the operational mass-flux convection scheme (Tiedtke, 1989) instead of using alternative simpler schemes (Kuo scheme, Betts-Miller scheme). Recent papers from Kasahara et al. (1996) and Fillion and Errico (1997) have shown that, in the context of assimilation of precipitation rates, retrieved moisture profiles are highly dependent upon the convection scheme used.

However, concerning the representation of clouds and radiation, a number of simplifications have been necessary, at least at this stage. The radiation scheme is computationally expensive, and requires spatial and temporal samplings for operational purposes. Therefore, the adjoint of the operational code would be prohibitive. The temporal sampling implies that the interactions between clouds and radiation are not completly represented. Within a 3-hour window, clouds remain fixed. In the context of data assimilation and singular vectors, where the typical time window will be 24 hours, it seems better a priori to have a simplified radiation scheme but allowing interactions with clouds at every time step. Otherwise, the sensitivity of radiative fluxes to changes in cloudiness (through specific humidity and temperature) given by the linear model, will be of limited use in the full non-linear model. A prognostic cloud scheme (Tiedtke, 1993) was introduced in the operational model in April 1995. This scheme introduces additional variables for cloud cover, liquid and and ice water contents. The adjoint of this cloud scheme will only make sense when the additional prognostic variables are included in the control variable to be optimized. This raises too many technical and scientific issues for them to be examined in these preliminary studies.

In order to reduce the validation part of simplified parametrizations within the non-linear model, previous operational schemes have been chosen. The large scale condensation scheme and the diagnostic cloud scheme to be linearized are those operational before April 1995. The planetary boundary layer scheme has also been modified in order to express exchange coefficients as functions of the local Richardson number only (Louis et al., 1982). The Louis scheme has some known weaknesses, such as the lack of entrainment at the top of the mixed layer (Beljaars, 1995), but produces a unified scheme easier to linearize than the operational one (e.g. the iterative estimation of the Monin-Obukhov length).

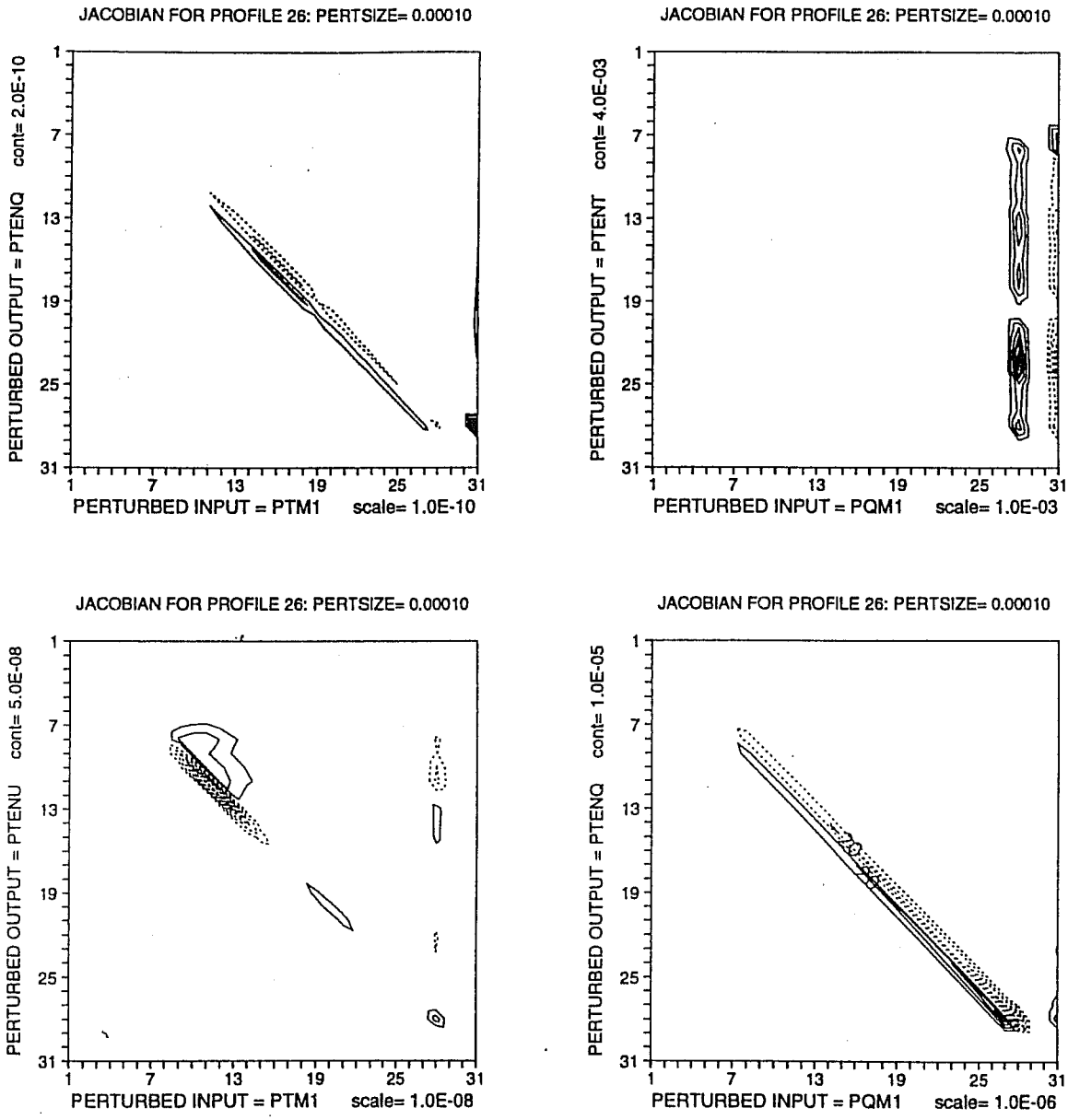

Figure 1: Jacobians for indicated pairs of input and output fields [PTM1=T, PQM1=q, PTENT=$\partial T/\partial t$, PTENQ=$\partial q/\partial t$] at model levels indicated on the ordinate and abscissa. The computation is for a profile having deep convection. The Jacobian is computed using perturbation of 10^{-4} K, $10^{-4}q_{sat}$ for T and q respectively. Contours intervals (indicated by cont= in the ordinate legend) are in terms of model units.

3.2 First set of linearized parametrizations

3.2.1 Vertical diffusion

A *vertical diffusion* scheme based on the use of the Richardson number dependency of the exchange coefficients (Louis et al., 1982) is applied everywhere in the atmosphere (surface boundary layer, planetary boundary layer, free atmosphere). Analytical expressions have been generalized for the situation of different roughness lengths for heat and momentum transfers. The mixing length profile uses the formulation of Blackadar (1962) with a reduction in the free atmosphere is order to avoid the computation of a planetary boundary layer depth.

3.2.2 Radiation

A simple *radiation scheme for the longwave* spectrum is based on a constant emissivity formulation. This approach requires the storage of emissivity arrays ε from the trajectory, but allows modifications of the fluxes with temperature (negative feedback). The tendency of the perturbed temperature can thus be written:

$$\frac{\partial T'}{\partial t} = -\frac{g}{C_p}\frac{\partial}{\partial p}\left(4\sigma\varepsilon T^3 T'\right) \tag{1}$$

3.2.3 Large-scale condensation

A *large scale condensation scheme* (classical moist adjustment scheme where all supersaturations are removed instantaneously as precipitation without the cloud stage), includes evaporation in subsaturated layers and snowfall melting.

3.2.4 Sub-grid scale orography

A parametrization of sub-grid scale orographic effects (*gravity wave drag*), represents the drag produced by low-level blocking and wave breaking according to Lott and Miller (1995).

3.2.5 Moist convection

The *convection scheme* is expected to have an impact on the quality of 4D-Var in the tropics. However, coding the tangent linear and adjoint versions of the ECWMF scheme represents a large amount of technical work. In order to examine rapidly the influence of convection on 4D-Var, an approach based on a simplified computation of the Jacobian matrices has been retained. The advantage of that method is to avoid an explicit coding of the tangent-linear and of the adjoint, while a major drawback is the computation and storage of huge arrays. This approach has been applied with success in mesoscale models (Lengland et al., 1996 ; Fillion and Errico, 1997). Diagnostic studies performed by Errico (1997) have shown that the Jacobian matrices

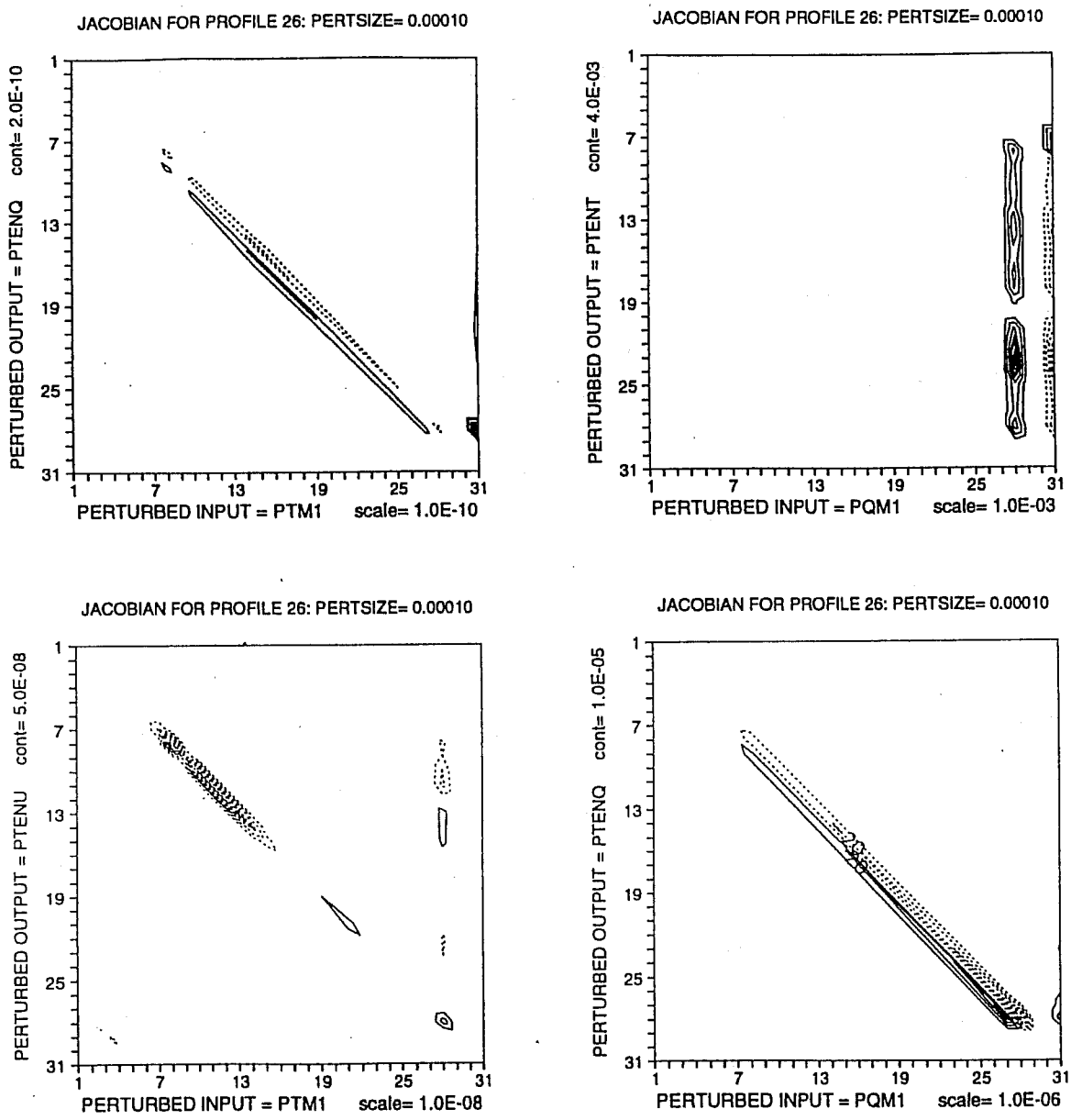

Figure 2: As Figure 1 but for approximate Jacobians

associated with the ECMWF convection scheme are rather sparse. Figure 1 shows that the sensitivity comes mostly from the surface and from the level just below cloud base. The diagonal part of the matrices corresponds to the mass flux transport. The strategy adopted consists in computing only a few columns (i.e. perturbed directions) and in reconstructing missing elements by interpolation/extrapolation. The cost corresponds to 12 calls of the non-linear convection scheme in the TL and AD versions of the IFS (instead of 125 for a full computation on a 31-level grid). No extra storage is required, and the approximated Jacobian matrices capture the main features of the full matrices (Figure 2). In this framework, modifications to the non-linear convection scheme (simplifications/regularizations) can easily be tested without any recoding (provided the structure of the Jacobian matrices is not fundamentally modified).

3.3 Evaluation of the non-linear parametrizations

Once some simplifications on the current operational parametrizations are devised, it is important to check that the quality of non-linear forecasts remains acceptable. The vertical diffusion scheme based on Louis et al. (1982) proposal and the diagnostic condensation scheme have been put back in a T106L31 version of the ECMWF model to perform a series a five 10-day forecasts. Since these parametrizations where previously in the operational ECMWF model, this validation does not need to be exhaustive. The model scores associated with the synoptic fields compares favourably with the reference, up to day 5 (Figure 3). However, prediction of weather elements (clouds, screen-level temperature) are in poorer agreement with SYNOP observations.

3.4 Evaluation of the linearized parametrizations

The linearity of the large scale condensation scheme has been tested by a comparison of linear and non-linear evolutions of a T42L31 version of the ECMWF model. The following Taylor formula is checked for various orders of magnitude of a given initial perturbation μx_0 :

$$\mathcal{M}_i(x_0 + \mu x_0) = \mathcal{M}_i(x_0) + \mu x_0 \cdot \mathcal{M}'_i(x_0) + \frac{\mu^2}{2} x_0^T \cdot \mathcal{M}''_i(x_0) \cdot x_0 + O(\mu^3) \qquad (2)$$

If ξ is the ratio of the non-linear evolution of a given perturbation over the linear one, by plotting $\log(\xi - 1)$ as a function of $\log(\mu)$, a straight line should be obtained for the range of perturbations associated with the linear regime. The original large scale condensation scheme does not present such behaviour, even if the accuracy of the tangent linear approximation reached for $\mu = 10^{-5}$ is very good (Figure 4) (results are presented for a given spectral coefficient of the specific humidity field). Relative error decreases when the size of the perturbation becomes smaller. For very small perturbations the relative error increases due to round-off errors. A quadratic smoothing has been introduced in the scheme around the saturation point (Figure 5). In that case, precipitation can be produced before reaching saturation in the grid-box (which is physically possible if one

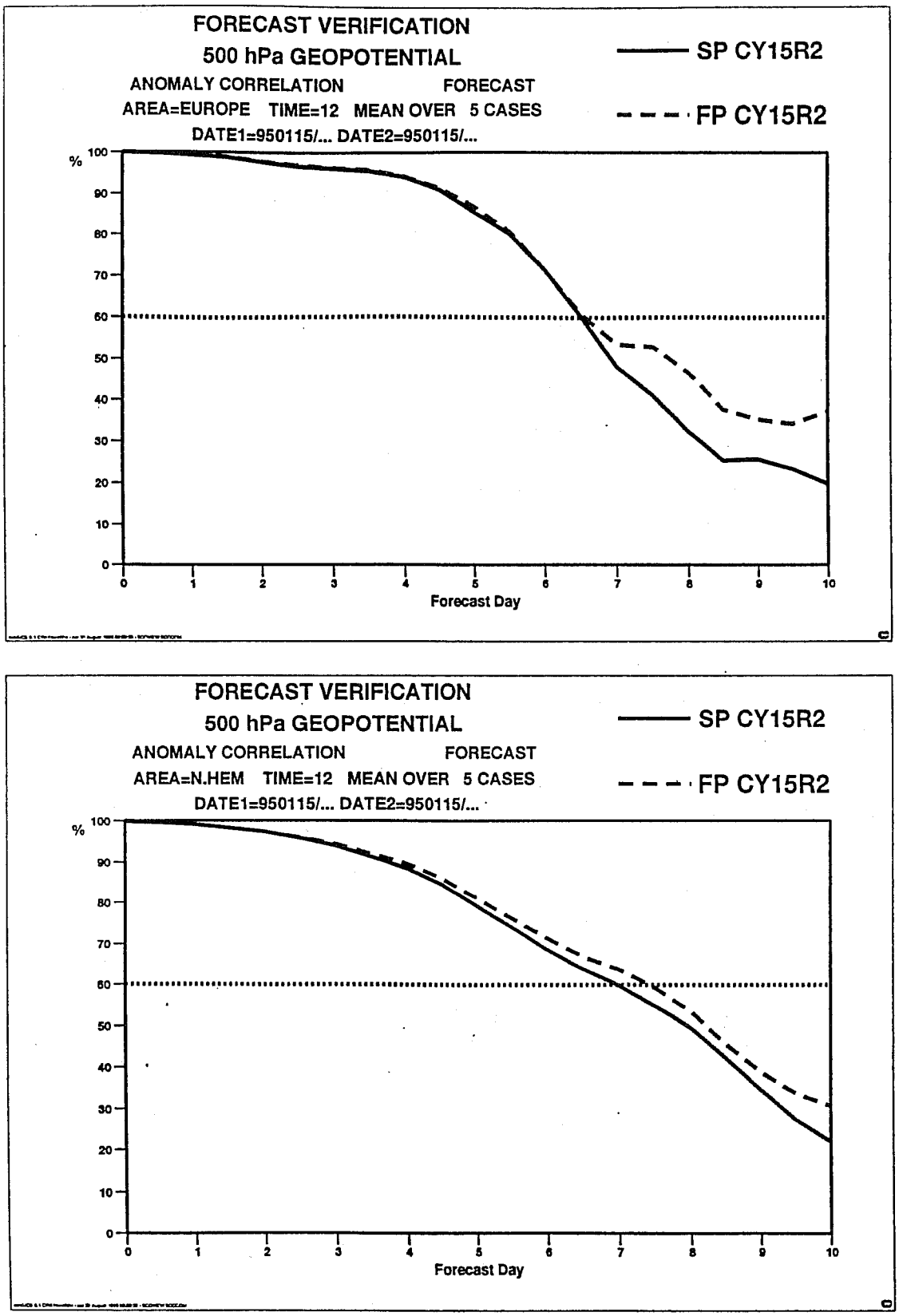

Figure 3: Mean anomaly correlation at 500 hPa height for T106L31 version with simplified physics [for linearization] (solid) and T106L31 version with operational physics (dashed) for Europe (upper) and extratropical Northern Hemisphere (lower) from 5 daily forecasts.

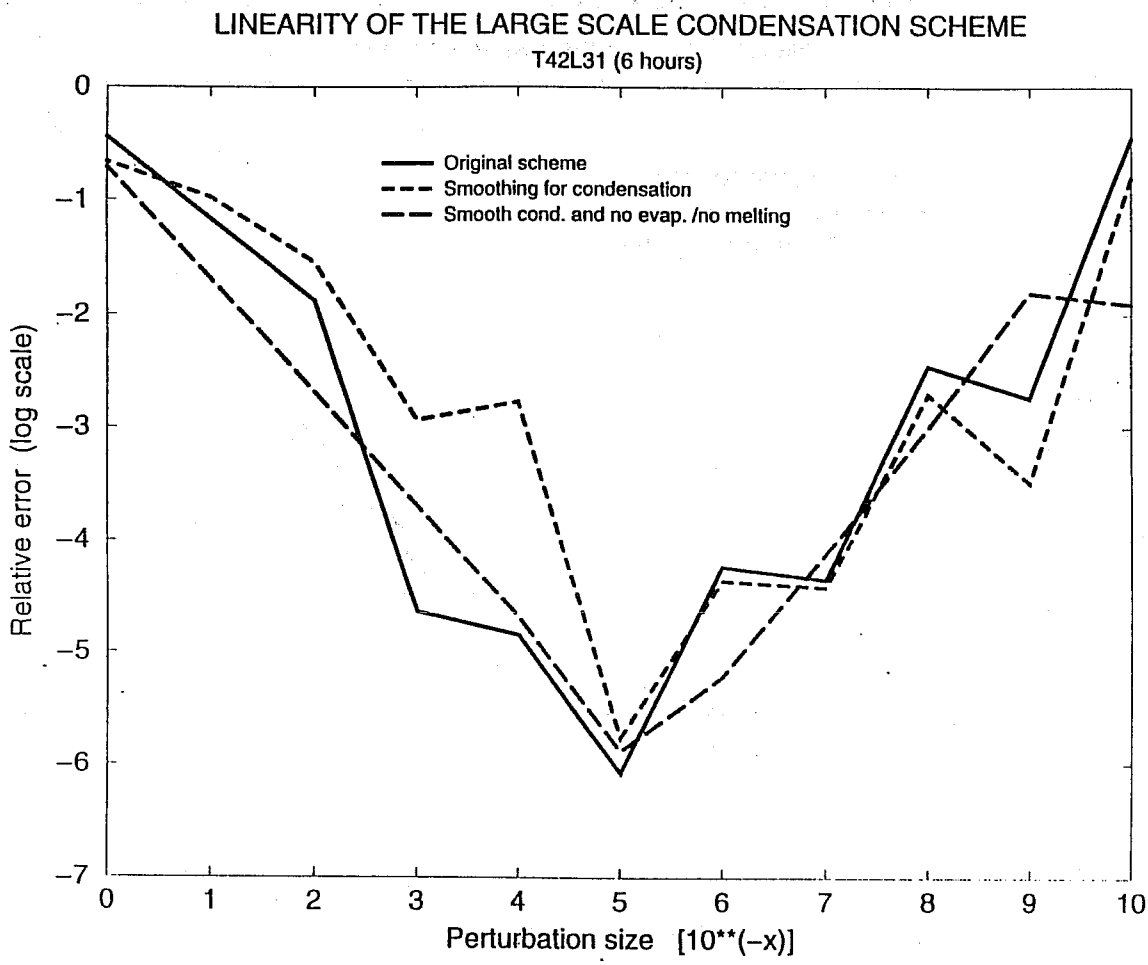

Figure 4: Linearity diagram of a spectral coefficient for specific humidity. The accuracy of the tangent-linear evolution with a model including large scale condensation is compared with pairs of non-linear integrations. The relative error after 6 hours is plotted in log-scale as function of the magnitude of the initial perturbation. The original scheme (solid) is compared with regularized versions (dashed).

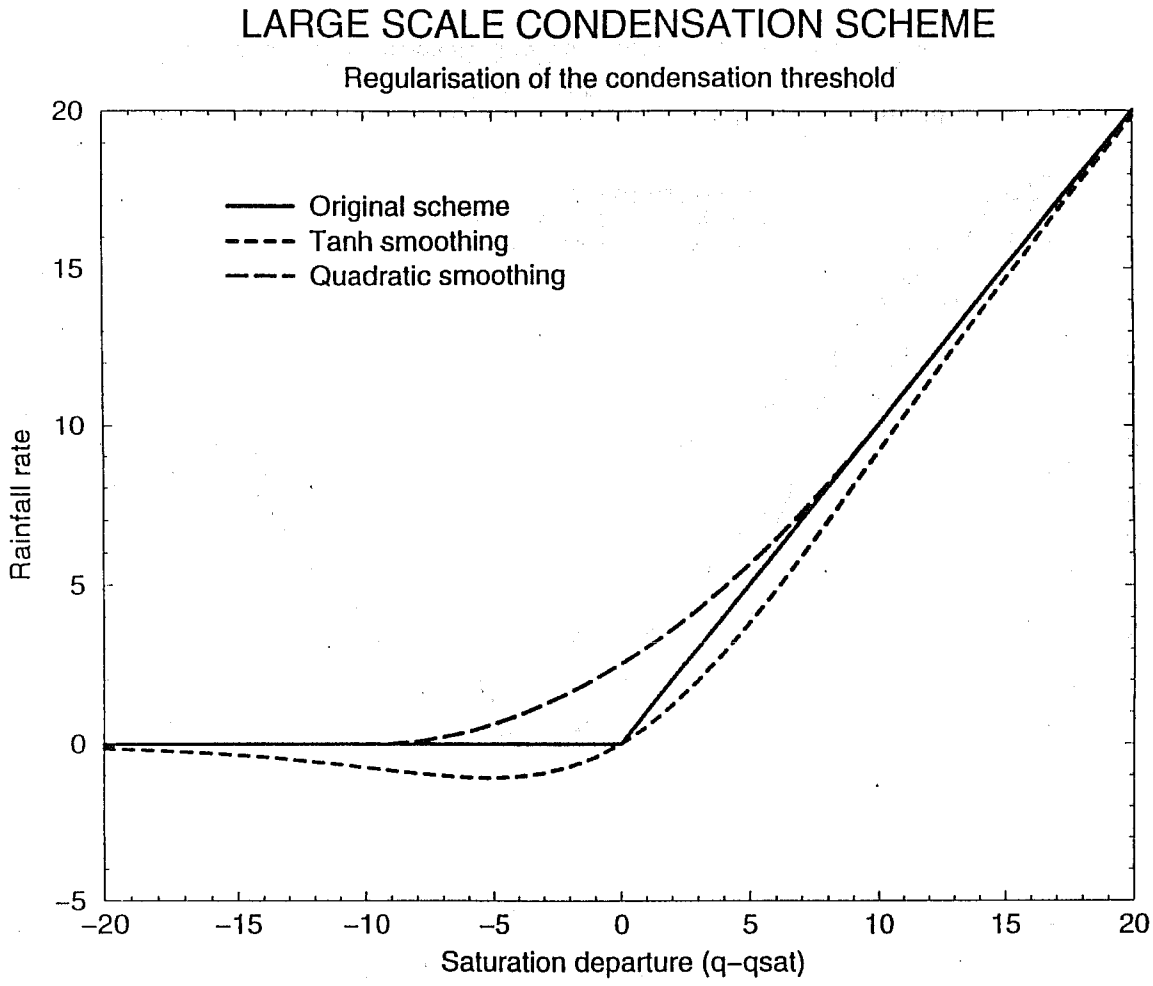

Figure 5: Grid-scale rainfall rate produced by the large scale condensation scheme as function of the difference $q-q_{sat}$ in arbitrary units. The initial switch (solid) $R = \alpha \max[0., q-q_{sat}]$ is regularized with a quadratic smoothing (long dashed) and an hyperbolic tangent smoothing (short dashed).

assumes a sub-grid scale statistical distribution of specific humidity). Figure 4 shows that the linearity range is only marginally increased. When also neglecting other physical processes defined with on/off switches (rainfall evaporation in subsaturated layers and snowfall melting) the linearity range extends over five orders of magnitude of the initial perturbation. Another type of smoothing was also tested for condensation by using an hyperbolic tangent function which is differentiable at all orders (Figure 5). This choice can lead to worse results (differentiability is increased but linearity is reduced), and spurious negative rainfall rates are estimated below saturation (water substance is not conserved).

The way rainfall evaporation reduces the linearity regime of the large scale condensation scheme can be understood by examining Jacobian matrices on Figure 6. Perturbations located along the diagonal are associated with a local increase of specific humidity q which enhances supersaturation, leading to more condensation (therefore $\partial q/\partial t$ decreases and thus $\partial \dot{q}/\partial q < 0$). This local excess of moisture has a remote effect below cloud base, producing more rainfall evaporation in the first subsaturated layer, thus $\partial \dot{q}/\partial q > 0$. When increasing the size of the moisture perturbation from 0.0001 to 1 (equivalent to 10% relative humidity), the shape of Jacobian matrices differs in places where thresholds are crossed. For profile 2, the low cloud layer extends further up by one level, and for profile 20, rainfall evaporation takes place in two layers.

Figure 7 summarizes the progressive reduction of validity of the tangent-linear approximation when going from an adiabatic model to a model including large scale condensation, gravity wave drag and vertical diffusion. When vertical diffusion is activated, the linearity regime is found for smaller sizes of perturbations than with the remaining physical processes.

The convection scheme cannot be tested using the ratio of model spectral coefficients between linear and non-linear integrations since the Jacobian approach only provides an approximate of the tangent-linear model. We have checked within the IFS that the tendencies (moisture sink Q_2 and heat source Q_1) produced by approximated Jacobians:

$$\left(\frac{\partial x'}{\partial t}\right)_{conv} \simeq \sum_{y=T,q,\dot{q}} \left[\frac{\Delta \dot{x}}{\Delta y}\right] y' \tag{3}$$

are close to the differences between two non-linear integrations of the convection scheme in the limit of very small perturbations. A good agreement is obtained as shown on Figure 8 for two columns characterized by deep and shallow convections.

Using only the full non-linear model, preliminary experiments were undertaken to examine the linearity of the convection scheme. For a given situation (10 September 1993 ; Floyd case) the T106L31 ECMWF model was run for short range forecasts (48 hours), various initial perturbed states $x_0 + \lambda \delta x_0$ are applied to the model $\mathcal{M}$. If the linear hypothesis is valid, for each value of

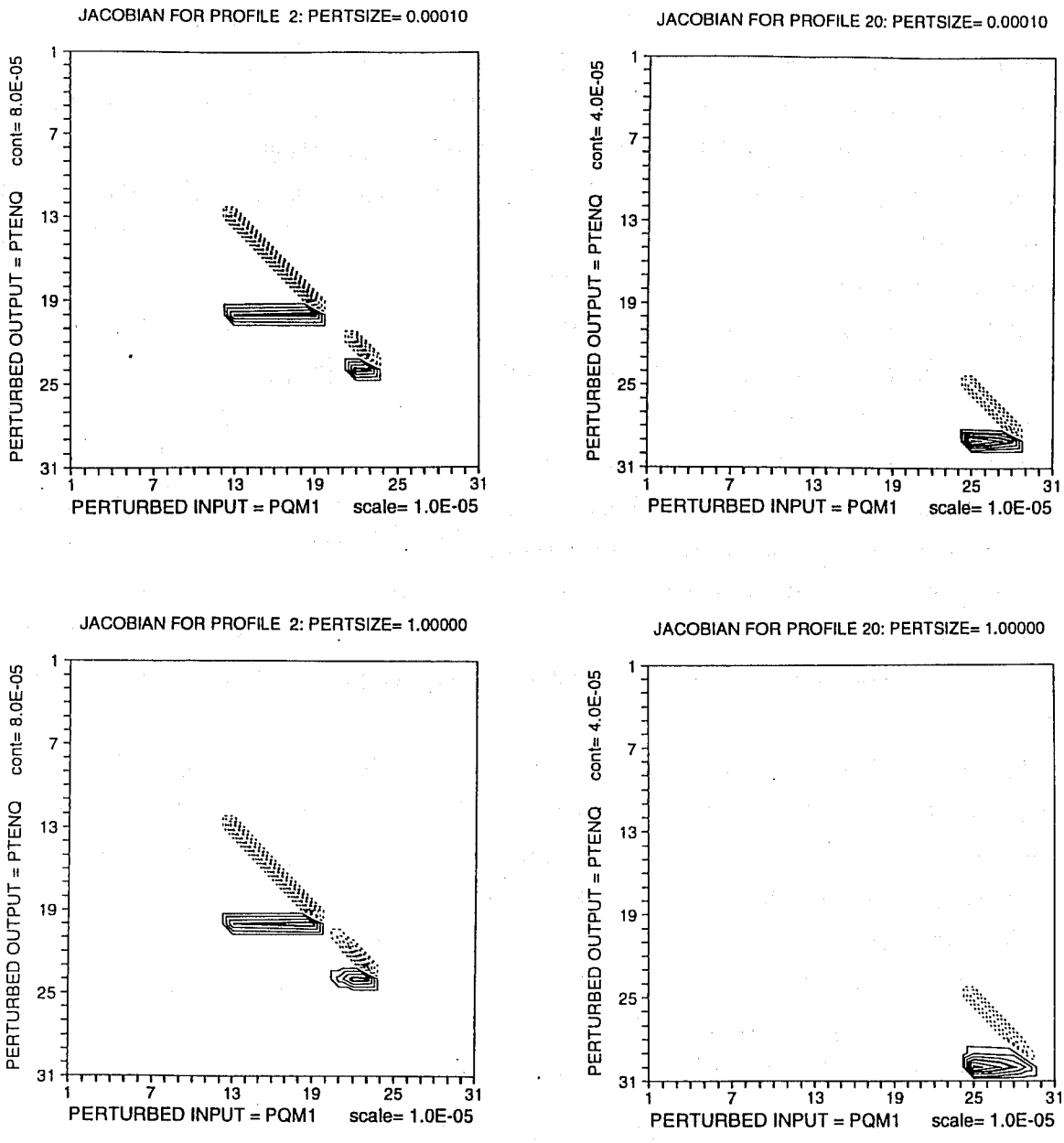

Figure 6: Linearity regime of Jacobian matrices ($\partial\dot{q}/\partial q$) for the large scale condensation scheme. The reference perturbation size 10^{-4} (upper panel) is increased by 10^4 (lower panel).

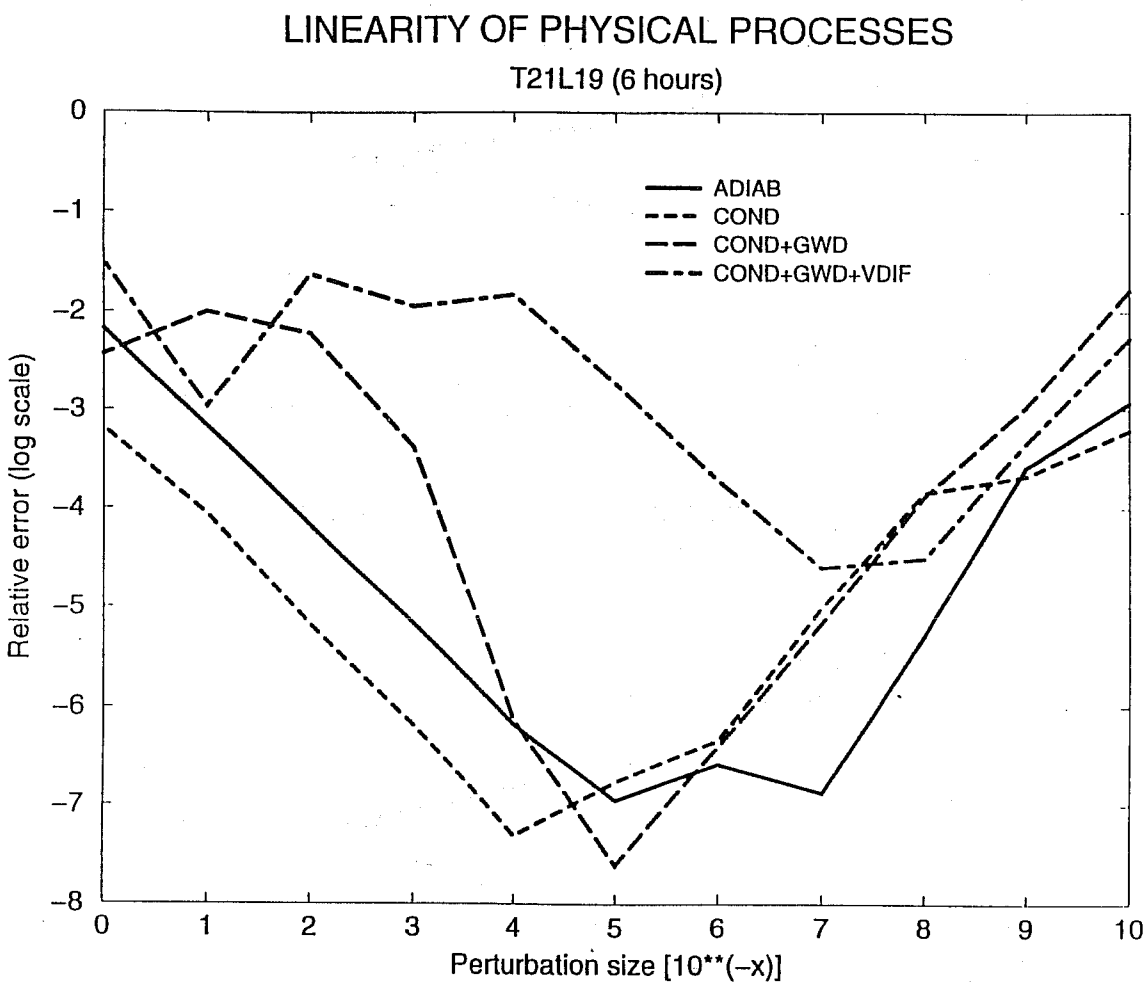

Figure 7: Linearity diagram of a spectral coefficient for temperature in T21L19 versions including various physical parametrizations (ADIAB=no physics ; COND=large scale condensation ; GWD=sub-grid scale orography ; VDIF=vertical diffusion). The accuracy of the tangent-linear evolution is compared with pairs of non-linear integrations. The relative error after 6 hours is plotted in log-scale as function of the magnitude of the initial perturbation.

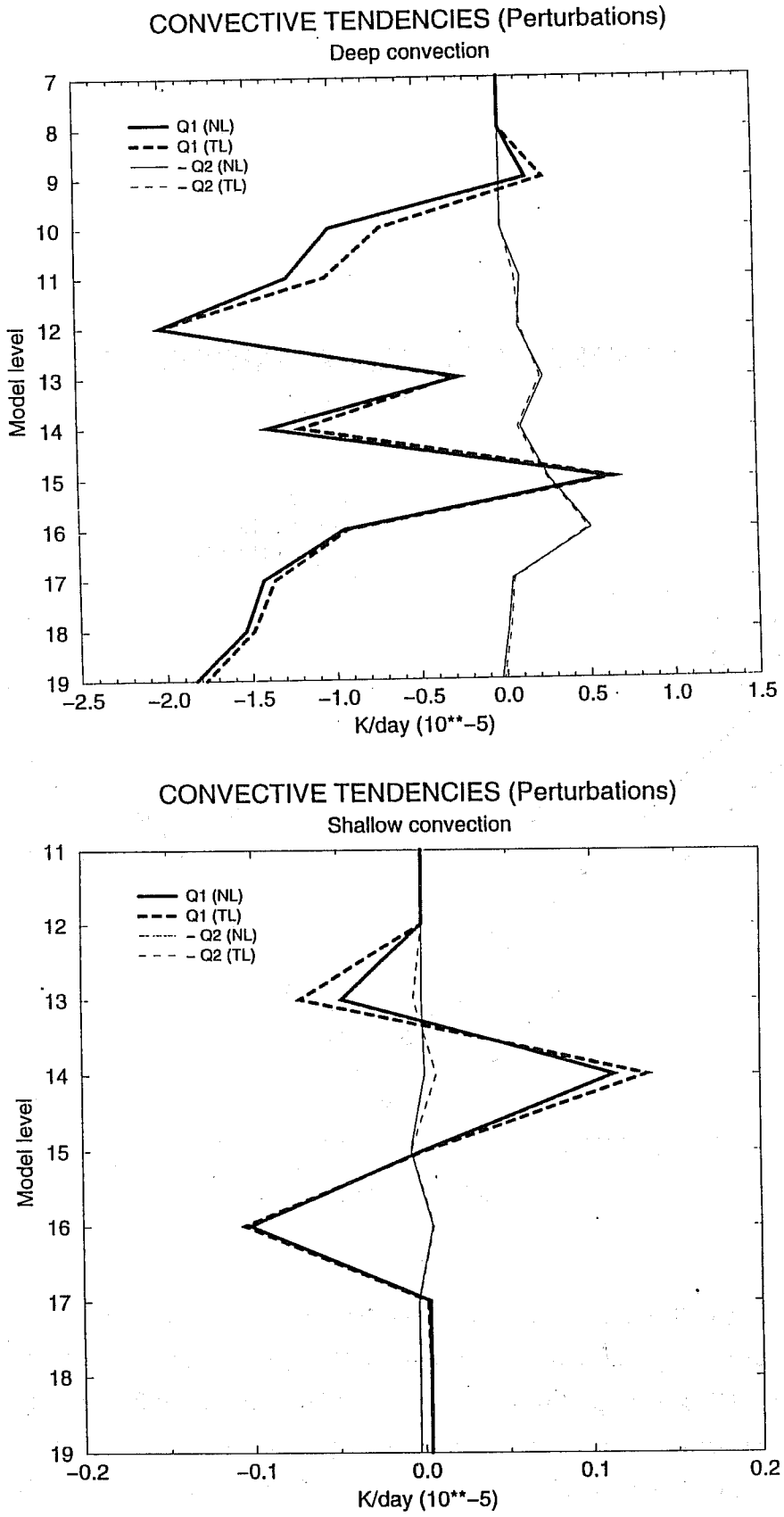

Figure 8: Perturbations of convective moisture and temperature tendencies ($Q1$ and $-Q2$ on the legend) produced from differences between two non-linear model integrations (NL on the legend) compared with the tangent-linear model using approximate Jacobians (TL on the legend) for a deep convection point (upper) and a shallow convection point (lower)

the parameter λ, the following equality should apply :

$$\lambda \times [\mathcal{M}(x_0 + \delta x_0) - \mathcal{M}(x_0)] = \mathcal{M}(x_0 + \lambda \delta x_0) - \mathcal{M}(x_0) \tag{4}$$

The initial perturbation δx_0 has been chosen from a sensitivity study described in Rabier et al. (1996). Perturbed fields are initially located above 30 N with a maximum amplitude of 0.5 hPa for the surface pressure (Figure 9). Simulations have been undertaken with λ ranging from 0.125 to 8 with and without the convection scheme. The linearity diagram for the maximum error of surface pressure after 12 h of simulation shows that the behaviour of the model is almost linear with and without the convection scheme (Figure 10a). The convection scheme however produces a non-linear behaviour for perturbations of very small initial amplitude ($\lambda = 0.125$). It appears that convection can be triggered at some places with a very rapid growth rate. The amplitude of these perturbations is almost independent of the magnitude of the initial perturbation and rapidly saturate with a low level of energy. The consequence is that they are hidden either when dealing with larger initial perturbations or when examining results after 24h where the initial perturbations associated with the baroclinic instability have grown enough to dominate the global signal (Figure 10b). Figures 11, 12 and 13 present 12h forecasts for perturbations of the surface pressure field with values of λ equal to 0.125, 1 and 8 respectively and normalized by $1/\lambda$. All fields look similar (which supports the linearity of the model) with significant perturbations located over the Northern Atlantic and Pacific oceans, except for $\lambda = 0.125$ with convection, where small scale perturbations dominate along the tropical belt. This study seems to indicate that the most critical parametrization for linearization is the convection scheme. However, the magnitude of the perturbations where non-linearities take place is perhaps too small (with respect to analysis errors) to be important for practical applications. Further diagnostics need to be done to address this question more completely.

4 Singular vectors with improved physics

The generation of effective perturbations is one of the major problems in Ensemble Forecasting. At ECMWF they are obtained by perturbing the initial conditions along the most unstable directions of the phase space of the system: the singular vectors.

The solution x of the model equations linearized about a non-linear trajectory:

$$\frac{dx}{dt} = \mathcal{M}'_l x \tag{5}$$

may be written as :

$$x(t) = L(t_0, t)x_0 \tag{6}$$

where L is the linear forward propagator, the time $t - t_0$ is called the optimization time interval, and $\mathcal{M}'_l$ is an approximation of the tangent-linear version of the ECMWF model $\mathcal{M}$. Specifically,

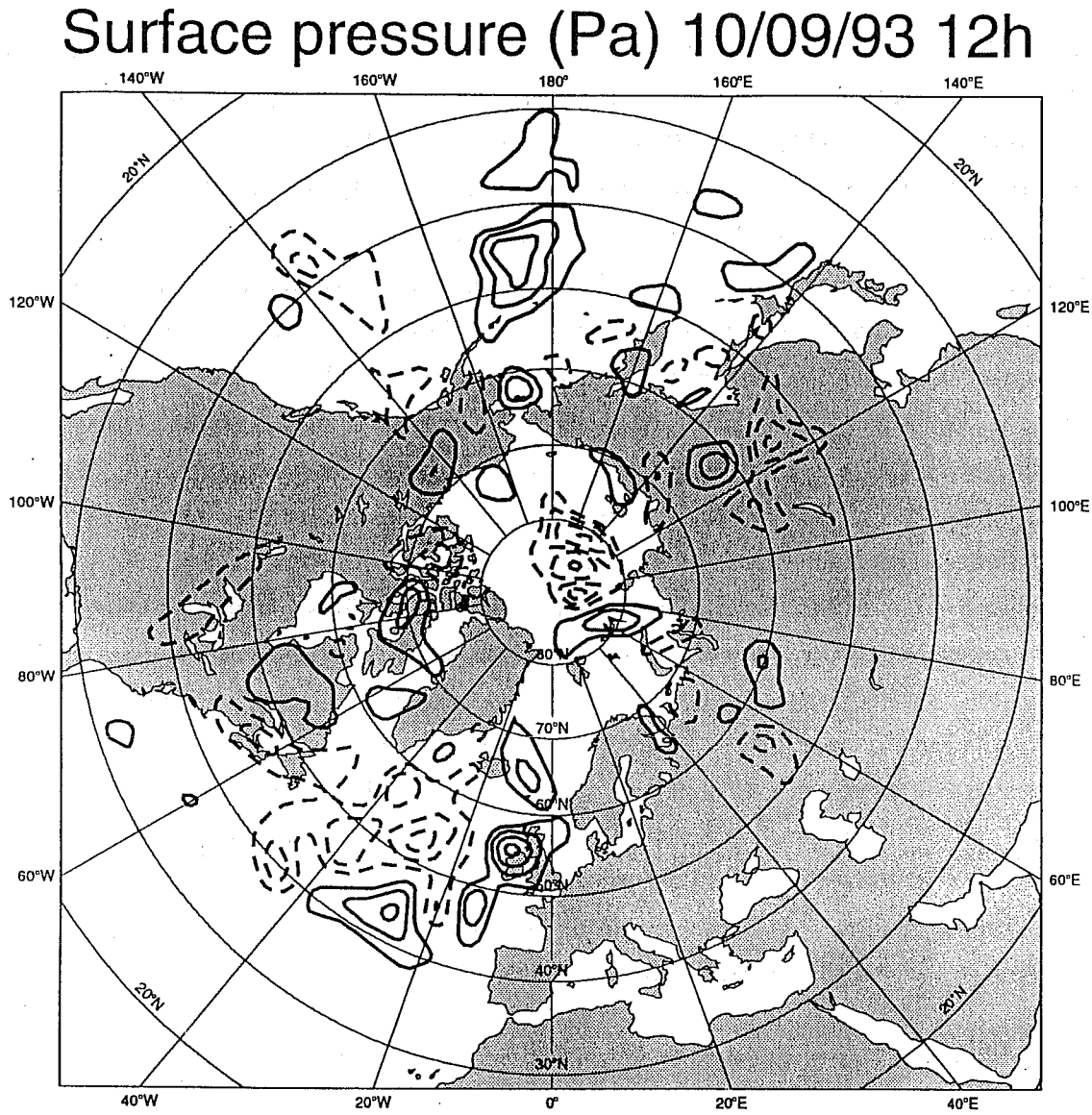

Figure 9: Initial perturbation of surface pressure for 10/09/93 at 12 Z computed from a sensitivity experiment (Rabier et al., 1996). Contour intervals are 25 hPa and dashed isoligns represent negative values.

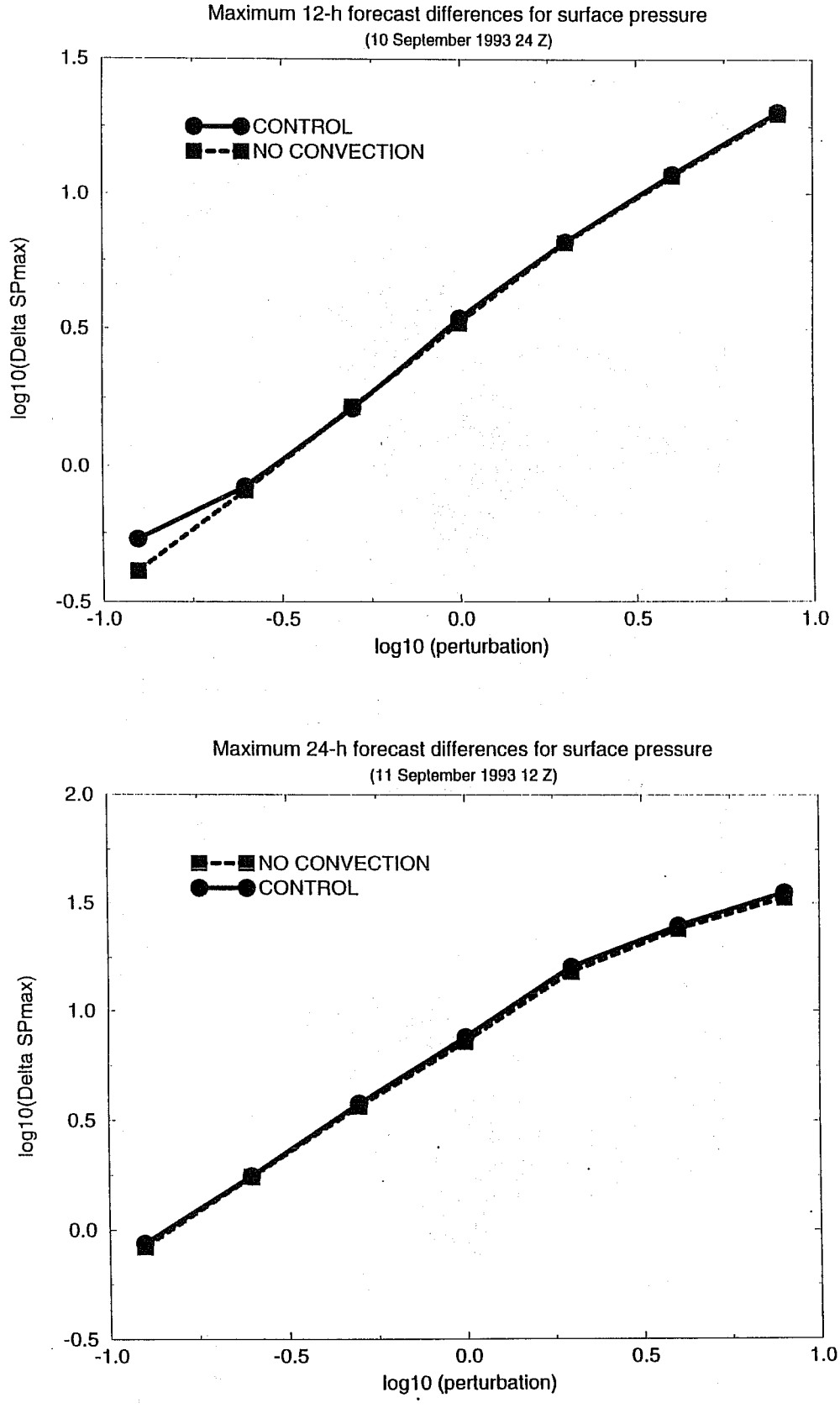

Figure 10: Maximum forecast differences of surface pressure in log-scale as function of the initial perturbation size λ in log-scale after 12 h (upper) and 24h (lower) with a T106L31 version of the ECMWF model with and without moist convection.

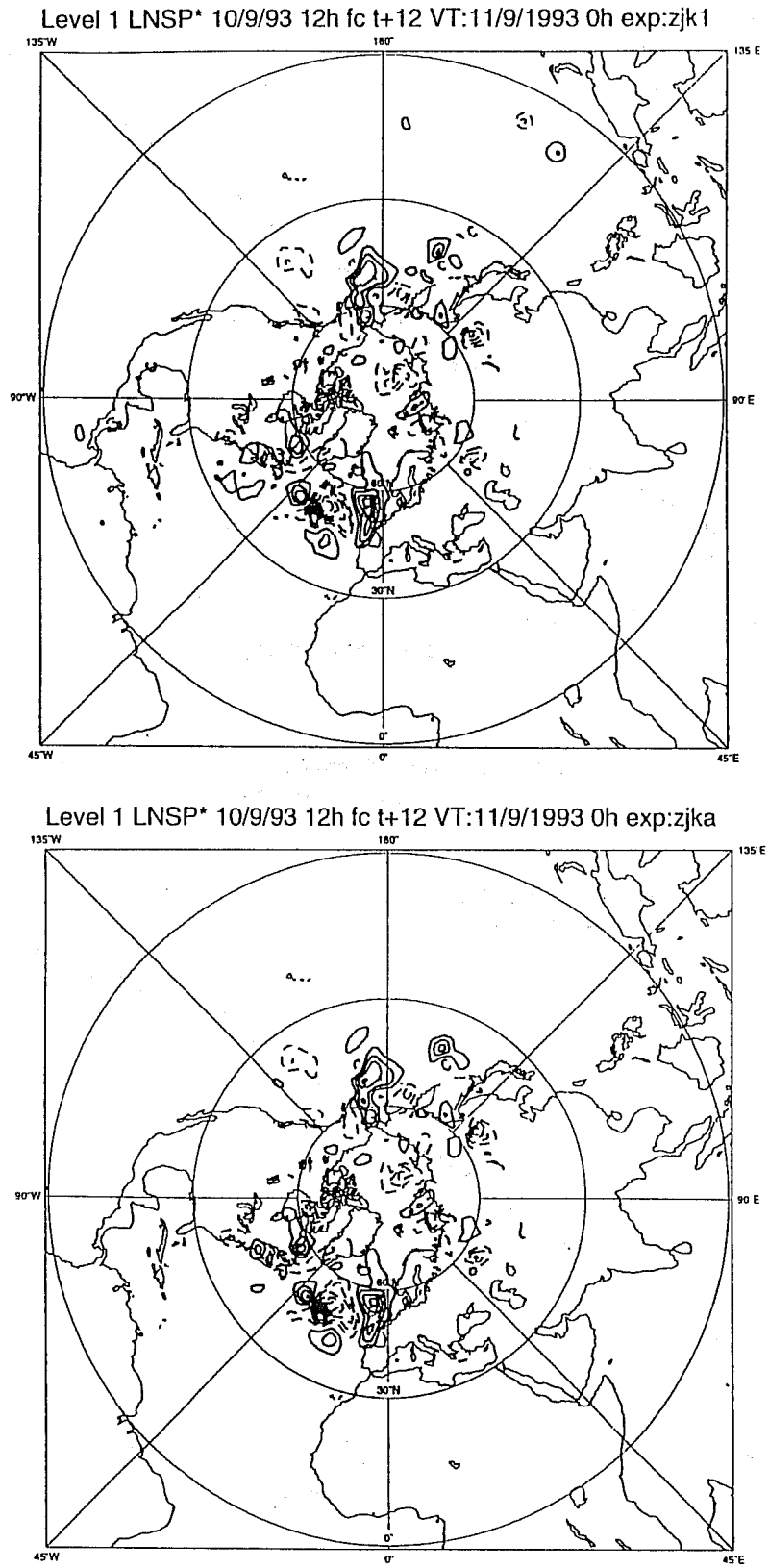

Figure 11: Evolution of the surface pressure perturbation shown on Figure 9 after 12-h forecast with a scaling factor $\lambda = 1$.

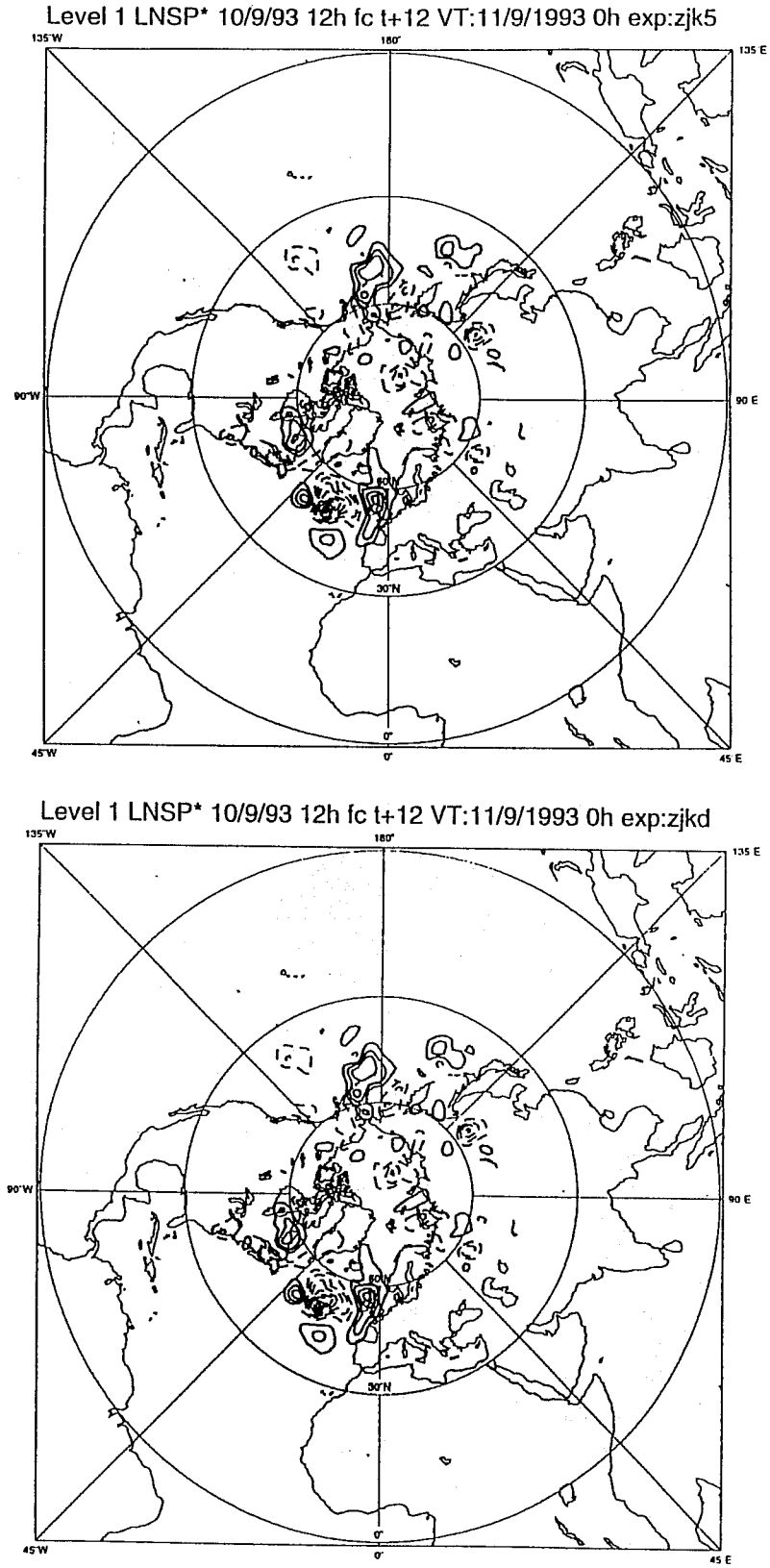

Figure 12: As Figure 11 with a scaling factor $\lambda = 8$ (increase by a factor of 8 of the initial perturbation).

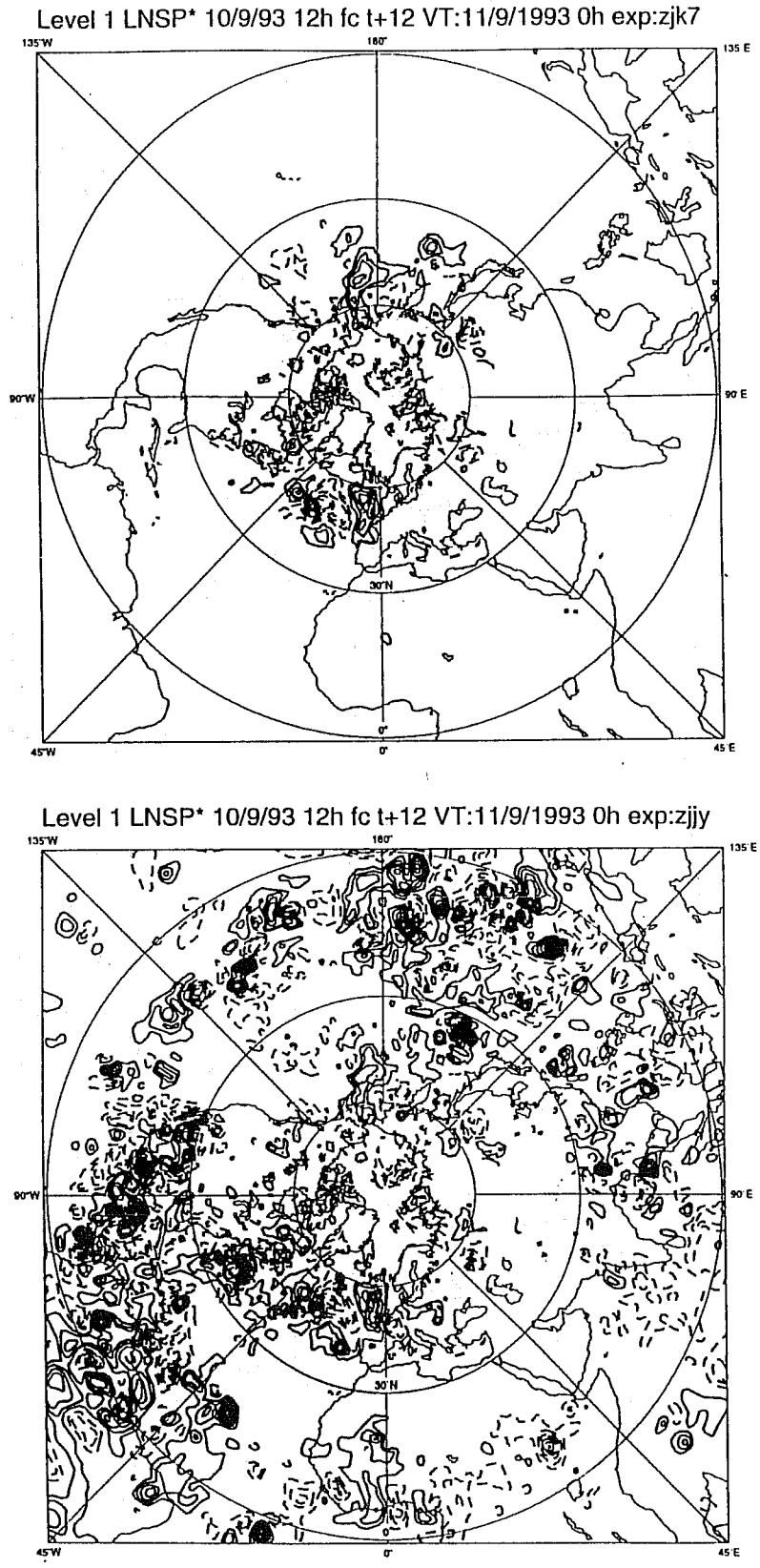

Figure 13: As Figure 11 with a scaling factor $\lambda = 0.125$ (decrease by factor of 8 of the initial perturbation).

the (linear) forward propagator is the product of operators representing large-scale condensation (L_{LSC}), vertical diffusion (L_{VDF}), adiabatic processes (L_{DYN}) and non-linear normal mode initialization (L_{NNMI}):

$$L = (\prod_{t_0}^{t} L_{LSC} L_{VDF} L_{DYN}) L_{NNMI} \tag{7}$$

Denote by $(.;.)$ an inner product based on total energy:

$$\begin{aligned}(x_1; x_2) \;=\; & \frac{1}{2}\int_0^1 \int_s \left(\nabla\Delta^{-1}\zeta_1 \cdot \nabla\Delta^{-1}\zeta_2 + \nabla\Delta^{-1}D_1 \cdot \nabla\Delta^{-1}D_2 + \frac{C_p}{T_r} T_1 T_2 + w_q \frac{L_v^2}{C_p T_r} q_1 q_2 \right) \\ & d\Sigma \left(\frac{\partial p}{\partial \eta}\right) d\eta + \frac{1}{2}\int_s R_d T_r P_r \ln(\pi_1)\ln(\pi_2) d\Sigma\end{aligned}$$

where ζ stands for vorticity, D for divergence, T for temperature, q for specific humidity, π for surface pressure, C_p is the specfic heat of dry air at constant pressure, L_v is the latent heat of condensation at 0 °C, R_d is the gas constant for dry air, $T_r = 300\ K$ is a reference temperature, and $P_r = 80000\ Pa$ is a reference pressure. Note that the parameter w_q defines the relative weight given to the humidity term [1].

The total energy of a perturbation x at time t can be computed as

$$||x(t)||^2 = (PLx_0; PLx_0) = (x_0; L^* P^2 L x_0) \tag{8}$$

where L^* is the adjoint of the linear propagator L with respect to the total energy scalar product $(.;)$ and P is the self-adjoint local projection operator (Buizza and Palmer, 1995). The application of the local projection operator permits the identification of singular vectors characterized by maximum growth rate over a selected region such as northern hemisphere (NH) above 30 N.

The singular vectors ν_j of the propagator LP are the perturbations with maximum localized energy growth over the optimization interval time $t - t_0$. They are computed solving the eigenvalue problem:

$$L^* P^2 L \nu_j = \sigma_j^2 \nu_j \tag{9}$$

Specifically, they are the eigenvectors ν_j with maximum eigenvalues σ_j^2 of the operator $L^* P^2 L$. The square root of an eigenvalue is called the singular value.

Singular vectors are computed for a case study (5 December 1994) at T42 spectral triangular truncation, with 19 vertical levels, for an optimization time of 48 hours. Four configurations are examined, either including or excluding the large scale condensation scheme, and assigning two different weights w_q to the specific humidity term in the total energy norm (Table 1).

[1] The moisture term is defined by assuming conservation of perturbed moist static energy in a condensation process $L_v q' = -C_p T'$.

Experiment	LSC scheme	w_q	σ_1
NOLSC.0	off	0.0	18.6
LSC.0	on	0.0	31.7
NOLSC.1	off	1.0	19.4
LSC.1	on	1.0	35.4

Table 1: Experiments list, with the growth rate of the leading singular vector

t=0	**NOLSC.0**	**NOLSC.1**	**LSC.0**	**LSC.1**
NOLSC.0	1.00	0.91	0.77	0.73
NOLSC.1		1.00	0.75	0.75
LSC.0			1.00	0.96
LSC.1				1.00

Table 2: Similarity indices computed among unstable sub-spaces of different experiments

We analyze first the impact of the weight parameter w_q on the singular vectors. The comparison of the **NOLSC.0** and **NOLSC.1** singular vectors shows that, when the large scale condensation is not used, the inclusion of the specific humidity term in the inner product has a very small impact on growth rates (Figure 14). A measure of the impact on singular vector structures is given by the similarity index of the unstable sub-spaces generated by the first 16 singular vectors, which measures the degree of parallelism between the two sub-spaces (two parallel unstable sub-spaces have similarity index 1.00, while two orthogonal sub-spaces have similarity index 0). Table 2 shows that the similarity index between the **NOLSC.0** and **NOLSC.1** is 0.91, indicating a high degree of parallelism. Similar conclusions can be drawn when considering experiments **LSC.0** and **LSC.1**, although a slightly stronger impact on growth rates and a slightly higher parallelism between the unstable sub-spaces can be detected.

We now focus on the experiments with $w_q = 1$ and examine the impact of the large scale condensation scheme. Figure 14 shows that large scale condensation processes increase the growth rates by 50 % with peaks of the order of 80 % for the leading vectors. Considering the singular vector structures, the scheme induces a shift of the total enegry spectra, at optimization time, towards higher wave numbers (Figure 15). Consequently, the structural change corresponds to a substantial reduction of the unstable subspaces parallelism (Table 2). For reference, the similarity index between the unstable sub-spaces generated by the first 16 singular vectors computed for consecutive dates and 48-hour optimization time is about 0.30.

It is worth mentioning the result of a more complete analysis of the sensitivity of singular vectors to the weight w_q , in the range $0.01 \leq w_q \leq 100$.

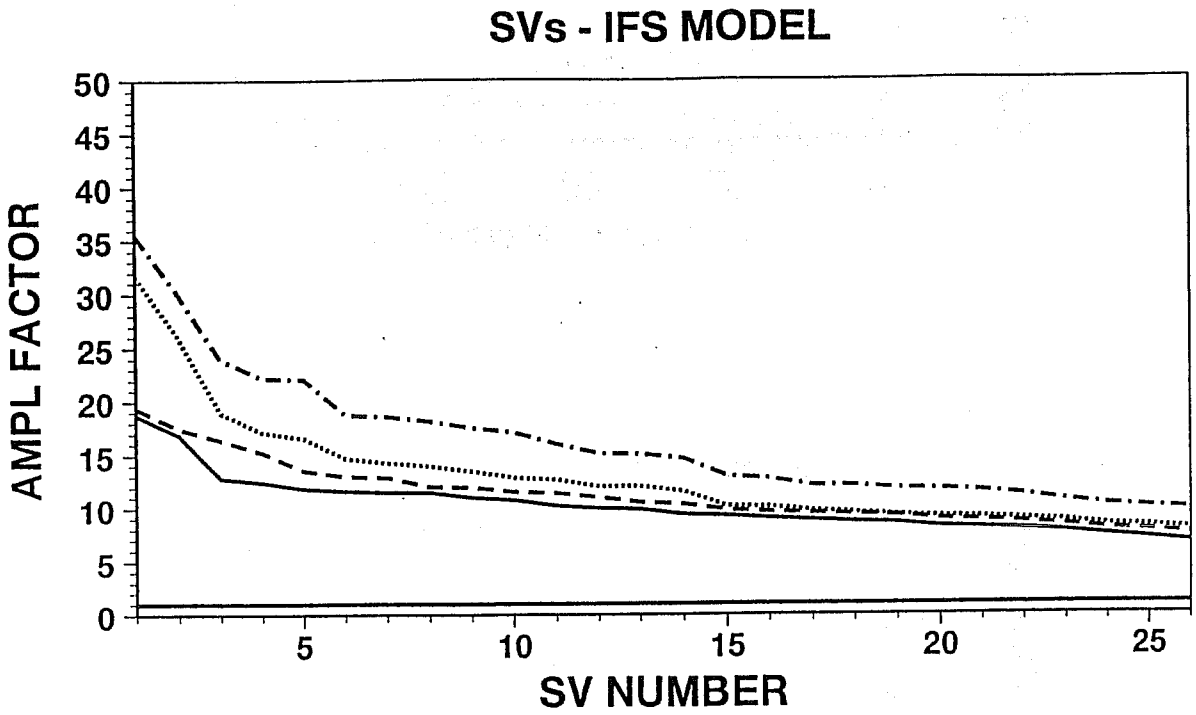

Figure 14: Growth rates of the first 26 singular vectors of experiments **NOLSC.0** (solid), **NOLSC.1** (dashed), **LSC.0** (dotted) and **LSC.1** (chain-dashed).

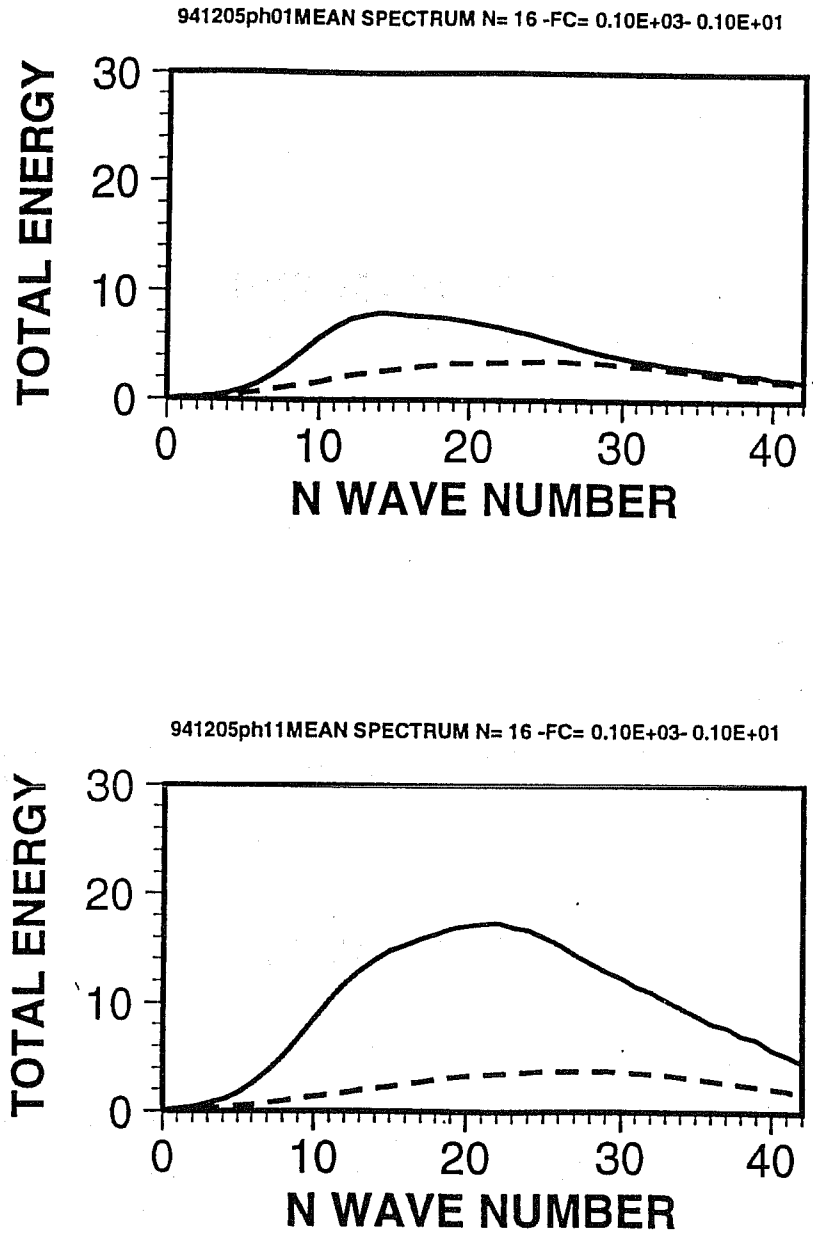

Figure 15: Mean total energy spectra at initial (dashed; increased by a factor of 100) and optimisation (solid) time, averaged among the first 16 **NOLSC.1** (upper) and **LSC.1** (lower) singular vectors.

If $w_q \ll 1$, at initial time the singular vectors have very large specific humidity component, and if the large scale condensation scheme is activated, growth factors much higher than **LSC.1** can be produced through latent heat release. In regions where the trajectory activates the condensation scheme, the large initial perturbations in moisture can be converted to temperature perturbations having a higher comparative weight in the scalar product definition. By contrast, if the large scale condensation is not active the impact on singular vectors is almost negligible, since there is no mechanism to transfer the moisture part of the total energy into its other components.

If however $w_q \gg 1$, the singular vectors are characterized by very small specific humidity components at initial time, and thus the activation of the large scale condensation scheme has very little impact. Nevertheless, growth rates much higher than **LSC.1** can be produced. The dynamics can increase the singular vectors' specific humidity component by the following mechanism: the perturbed wind field component V' is modified so that the perturbed specific humidity q' is increased by advection of the basic state specific humidity q, essentially through a contribution during the linear evolution of the term $V'.\nabla q$.

These results are in agreement with analytical and numerical studies of moist frontogenesis, where the development of a baroclinic wave is enhanced when latent heat release is accounted for in the ascending part of the frontal zone (Thorpe and Emanuel, 1985).

For a different situation (23/10/93) and a T42L31 version of the IFS, preliminary computations of singular vectors have been performed with all the physical processes linearized except the convection. The optimization period of 48 hours lead to unphysical growth of the singular vectors initially located in the tropics when convection is added. This result needs further investigation, but certainly indicates that the tangent-linear approximation is not valid anymore over a two day period when the forecast model includes moist convection. Results are summarized for the spectrum of the first 16 vectors (Figure 16). With respect to the reference (simplified diffusion), the improved vertical diffusion produces lower amplification rates although the shape of the spectrum is unchanged. The inclusion of the radiation and sub-grid scale orography has a small effect but also acts to damp the growth of the perturbations. Large scale condensation, as described above, increases the amplification rate of the most unstable perturbations.

5 Preliminary conclusions

A first set of linearized physical parametrizations has been devised for use in the tangent-linear and adjoint versions of the ECMWF forecast model. Given the time scale of interest for data assimilation and singular vectors (24 hours) the following processes are represented: vertical diffusion, gravity wave drag, large scale condensation, radiation, moist convection. Simplifications

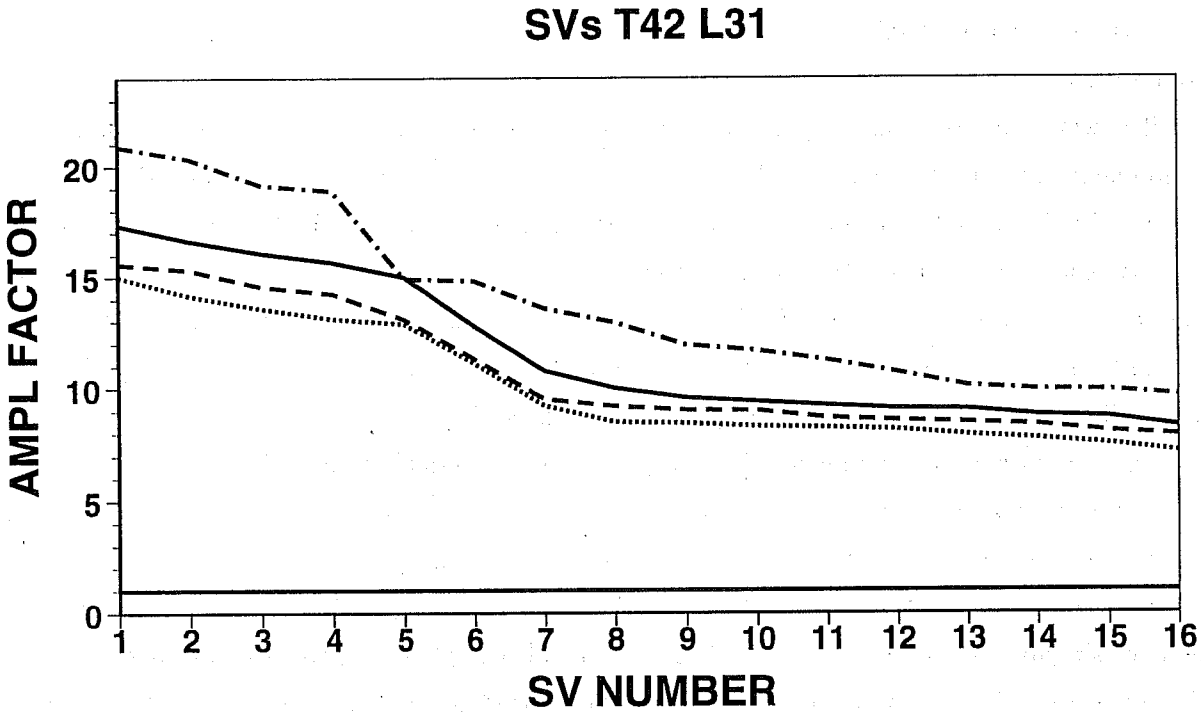

Figure 16: Growth rates of the first 16 singular vectors for T42L31 experiments (optimization time : 48 hours) with progressive inclusion of physical processes : Reference (solid); VDIF+RAD (dashed); VDIF+RAD+GWD (dotted); VDIF+RAD+GWD+COND (chain-dashed). [VDIF=vertical diffusion from Louis et al., RAD=simplified longwave radiation, GWD=sub-grid scale orography, COND=large scale condensation compared to a Reference (simplified vertical diffusion)].

with respect to the operational parametrizations have been defined in order to describe the main interactions between the processes. A priori, it seems better to represent most of the processes, even if some approximations are necessary, than to retain only a few physical processes with a high level of details.

As expected, the range of validity of the tangent-linear approximation is reduced when including physical processes in the model. Preliminary tests on singular vector computations showed that a more realistic vertical diffusion scheme produces results comparable to the simplified scheme devised by Buizza (1994). The inclusion of the large scale condensation parametrization scheme confirms the results of Ehrendorfer et al. (1996), that higher amplification rates can be achieved through latent heat release. Recent results from Langland et al. (1996) also show that moist processes contribute to a reinforcement of dry baroclinic instability. Moreover, our results indicate that the inclusion of large scale condensation processes induces a shift of the singular vectors' total energy towards larger wave numbers. Moist convection appears to be the most non-linear physical parametrization, therefore its use for computing unstable modes for large optimization periods could lead to unrealistically large growth rates. However, in the context of data assimilation, the 4D-Var incremental approach will help to deal with non-linearities. The sensitivity study of Rabier et al. (1997) as well as the empirical physical initialization techniques are very encouraging for the potential of physical processes to help to extract more efficiently information contained in observations (particularly in the tropics) in order to get improved analyses.

Concerning some technical issues mentioned in Courtier et al. (1994), it appears that automatic tools to produce adjoint codes are not yet reliable enough, and have not been helpful for coding the adjoint of the ECMWF physics. The linearized versions of the IFS still use an Eulerian time integration scheme. Therefore, the trajectory of model variables at $t - \Delta t$ is needed for the physics. It implies a doubling of memory storage that will be unnecessary when the adjoint of the two-time level semi-lagrangian scheme is developed. The ECMWF physics uses a fractional step method for updating the tendencies of the prognostic variables (Beljaars, 1991), which means that the actual amount of storage for the trajectory is increased by a factor of 3 since adiabatic tendencies are also required.

6 Future developments

6.1 Ideas for simplified radiation and convection schemes

Future developments will concern improvements of the linear radiation scheme and its interactions with clouds, and the convection scheme. Following ideas of Chou and Neelin (1996) a linear radiation scheme for the longwave part is being developed at ECMWF.

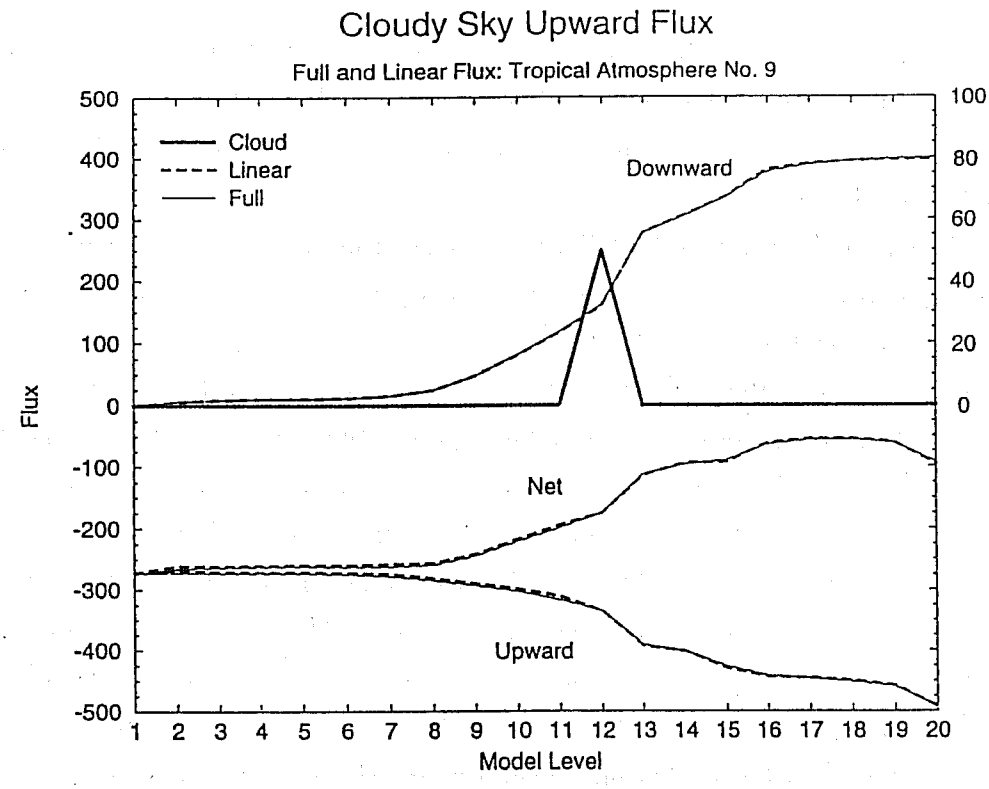

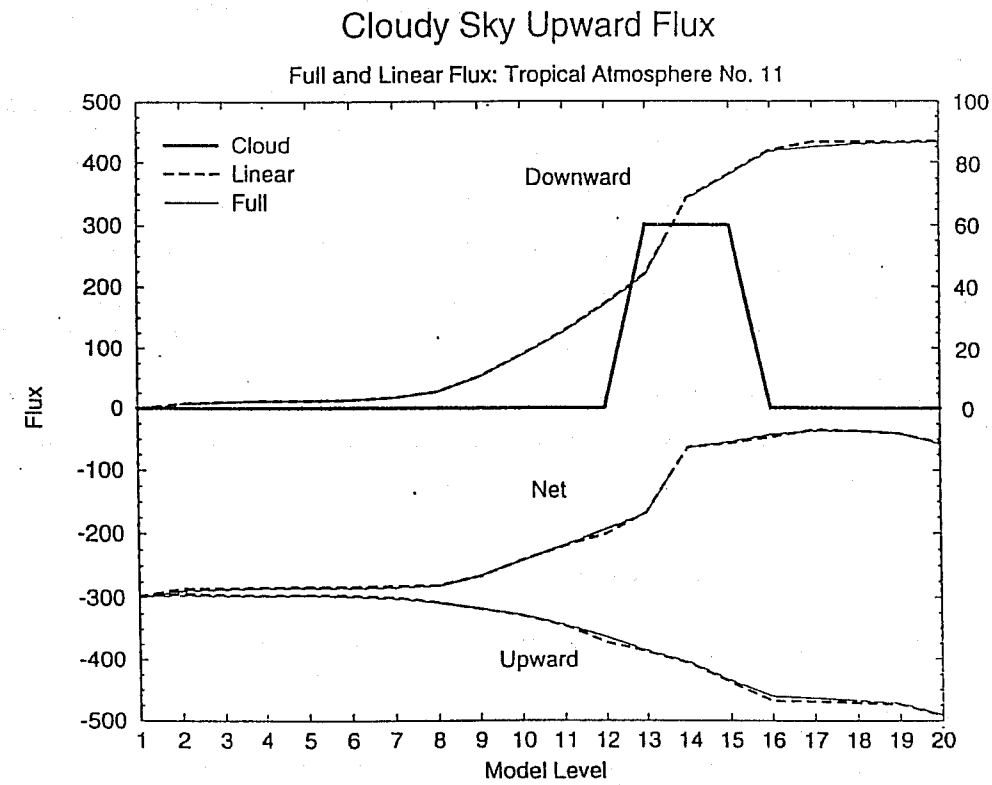

Figure 17: Vertical profiles of radiative fluxes for two cloudy tropical atmospheres obtained with the full ECMWF longwave radiation scheme and with a linearized version.

The longwave flux F (upward and downward) at a given level k is expressed by :

$$F(k) = < F(k) > + \sum_X \sum_{k'} \left\langle \frac{\partial F}{\partial X} \right\rangle (k,k') \{ < X(k') > - X(k') \} \qquad (10)$$

where $< X >$ is the zonal mean of X, being parameters to which longwave fluxes depend on (e.g. temperature and specific humidity profiles, surface pressure, ozone, ...). The Jacobian matrices $< \partial F/\partial X >$ are to be computed for both clear sky and cloudy atmospheres for a sample of latitude rows, by a perturbation method at the first model time step. One column simulations performed by J.-J. Morcrette for various sets of atmospheres show that the linear scheme compares favourably with the full radiation scheme (Figure 17).

Such a scheme could be used in data assimilation and called every time step and every grid point to allow full interactions with cloudiness. With such a scheme, the linearization of the previous operational diagnostic cloud scheme (Slingo, 1987) will make sense. Since the shortwave part is much less expensive, the linearization of the operational scheme is affordable.

Concerning moist convection, if it appears that the Jacobian approach has a positive impact on 4D-Var, it could be worth developing a simplified linearized convection scheme before handling the complexity of the full operational ECMWF scheme.

Since the very simple $\dot{\eta}$-relaxation proposed by Rabier et al. (1997) produced encouraging results, it may be possible to account for the effect of the cumulus induced subsidence in a more physical way. The experience with vertical diffusion for singular vectors (Buizza, 1993) has proved that simplified physical parametrizations can help to improve the realism of the tangent-linear model, even if only part of the processes are described (constant PBL depth, neutral stability only).

The apparent heat source Q_1 and moisture sink Q_2 produced by convection can be written as follows, when assuming cloud properties described by a bulk model (Tiedtke, 1989) :

$$Q_1 - Q_R = -\frac{1}{\rho}\frac{\partial}{\partial z}[M_u s_u + M_d s_d - (M_u + M_d)s] + L(c_u - e_d - e_l - e_p) \qquad (11)$$

$$Q_2 = -\frac{1}{\rho}\frac{\partial}{\partial z}[M_u q_u + M_d q_d - (M_u + M_d)q] - (c_u - e_d - e_l - e_p) \qquad (12)$$

where $s = C_p T + gz$ is the dry static energy, q the specific humidity, ρ the density of air, M_u, M_d, c_u and e_d are the net contributions from clouds to the upward mass flux, downward mass flux, condensation and evaporation, respectively, and s_u, s_d, q_u and q_d are the weighted averages of s and q from all updrafts and downdrafts. Here e_l is the evaporation of cloud air that has been detrained into the environment and e_p is the evaporation of precipitation in the unsaturated subcloud layer.

Using the equations of the bulk cloud model for both cumulus updrafts and downdrafts, the

Q_1 and Q_2 can be rearranged as:

$$Q_1 - Q_R = \frac{1}{\rho}\left[(M_u + M_d)\frac{\partial s}{\partial z} + D_u(s_u - s) + D_d(s_d - s)\right] - L(e_l - e_p) \quad (13)$$

$$Q_2 = \frac{1}{\rho}\left[(M_u + M_d)\frac{\partial q}{\partial z} + D_u(q_u - q) + D_d(q_d - q)\right] + (e_l - e_p) \quad (14)$$

The first term accounts for the compensating subsidence induced by cumulus convection (warming and drying) and the second one represents the detrainment of cloud properties in the environment. The last terms are the cooling and moistening from cloud and precipitation evaporation. In deep convective situations, the first term is the dominant one for Q_1 and also for Q_2 in the upper part of the cloud (Yanai et al., 1973 ; Gregory and Miller, 1989).

The difficult part of the linearization concerns the perturbation of cloud properties. On the other hand, the trajectory at $t - \Delta t$ being available in the TL/AD versions of the IFS, the mean properties of convection can easily be computed. The simplest way to linearize the convection scheme is to assume that cloud properties are constant and to account only for their effect on the perturbed fields describing the environmental properties:

$$Q'_1 - Q'_R = \frac{1}{\rho}\left[(M_u + M_d)\frac{\partial s'}{\partial z} - (D_u + D_d)s'\right] \quad (15)$$

$$Q'_2 = \frac{1}{\rho}\left[(M_u + M_d)\frac{\partial q'}{\partial z} - (D_u + D_d)q'\right] \quad (16)$$

This simplification retains the dominant term : the "pseudo-vertical advection" by convection of the perturbed fields, which almost cancels the "mean adiabatic vertical advection". The mass-fluxes M and the detrainment rates D are provided by a non-linear computation of the full convection scheme.

Such an approach retains some of the effects of convection, similar to what Rabier et al. (1997) tried to represent when reducing the vertical velocity in the tropics. However, the magnitude of the mass-flux can vary spatially and temporally. The present approach accounts for such variations by only operating on convective points diagnosed for the trajectory.

This approach represents a dominant process for deep convection (diagonal part of the Jacobian matrices described on Figure 1) but may be less suited for shallow convection where detrainment processes at cloud top dominate. However it is simple enough to be tried rapidly, and can be seen as a first step towards the full linearization of the ECMWF convection scheme.

The explicit coding of the adjoint of the full convection scheme will be required when assimilation experiments using observed precipitation are to be performed.

6.2 Towards the assimilation of precipitation rates using microwave radiances

There are several possible options for performing a variational assimilation of microwave radiances. Variational techniques require the adjoint of a transfer model between observations and

model variables (observation operator) in order to provide an efficient estimate of the gradient of the cost-function to be minimized. They extract in an optimal way the signal contained in available observations knowing a background information (6-h forecast).

A 1D-Var assimilation of SSM/I radiances has been developed by Phalippou (1996) using the adjoint of a microwave radiative transfer model. This technique allows retrieval of specific humidity and liquid water profiles and surface wind speed. This transfer model can be adapted to account for rainfall rates profiles.

The adjoint of the moist physical parametrizations (deep convection, grid scale precipitation) allows the fitting of temperature and specific humidity profiles in order to match observed precipitation rainfall rates, as shown in a feasibility study by Fillion and Errico (1997).

In a first stage, a 1D-Var assimilation using the adjoint of the ECWMF moist physics and a statistical relation between brightness temperatures and rainfall rates (e.g. Ferraro et al., 1996) could be performed. In that context, it is possible to use the framework of the 1D-Var satellite retrievals developed at ECMWF for TOVS and SSM/I to order to get the collocation of the first-guess and information on background error statistics (Andersson et al., 1993). The difficulty of such exercise is the specification of observation error statistics for the retrieved rainfall rates (and also bias corrections and quality control). The second step is to develop a coupled 1D-Var assimilation using both the physical parametrizations and the radiative transfer model. The specification of observation errors is then easier (mostly instrumental errors). Optimal profiles of moisture and temperature can be derived from a minimization algorithm in order to match observed radiances, given a background constraint. The coupling will take place through the rainfall rate profiles, being the output of the moist parametrizations and the input of the radiative transfer model.

A 1D-Var assimilation of radiances for retrieving rainfall rate profiles could also be possible in principle. However, a number of difficulties exists with this approach, namely the collocation of rainfall rate profiles for the first-guess (spatial and temporal interpolation), the estimation of background errors for these quantities, the estimation of 'pseudo-observation' errors of the retrieved profiles.

The 1D retrieved profiles will be introduced in the 3D-Var or 4D-Var assimilation system in a way to be defined (direct profiles, total precipitable water column). The next step will be to perform a direct 4D-Var assimilation (horizontal and temporal consistency, use of all types of data simulaneously). The impact of the use of such data will be assessed on both the analyses and the forecasts.

Acknowledgements

We would like to thank Mats Hamrud and Lars Isaksen for their technical support in implementing the trajectory management for the physics within the IFS. Discussions with our colleagues from the Physics section have been very useful in defining the first package of linearized physical parametrizations. Adrian Simmons, Martin Miller and Anton Beljaars provided useful comments on the manuscript.

References

Andersson, E., J. Pailleux, J.-N. Thépaut, J.R. Eyre, A.P. McNally, G.A. Kelly, and P. Courtier, 1993: Use of radiances in 3D/4D variational data assimilation. In *ECMWF Workshop on Variational assimilation with emphasis on three-dimensional aspects*, pages 123–156, Shinfield Park, Reading (UK). ECMWF. 9-12 November 1992.

Beljaars, A.C.M., 1991: Numerical schemes for parametrizations. In *ECMWF Seminar on Numerical methods in atmospheric models*, pages 1–42, Shinfield Park, Reading (UK). ECMWF. 9-13 September 1994.

Beljaars, A.C.M., 1995: The impact of some aspects of the boundary layer scheme in the ECMWF model. In *ECMWF Seminar on Parametrization of sub-grid scale physical processes*, pages 125–161, Shinfield Park, Reading (UK). ECMWF. 5-9 September 1994.

Blackadar, A.K., 1962: The vertical distribution of wind and turbulent exchange in a neutral atmosphere. *J. Geophys. Res.*, **67**, 3095–3102.

Bouttier, F., 1993: The dynamics of error covariances in a barotropic model. *Tellus*, **45A**, 408–423.

Buizza, R., 1993: Impact of simple vertical diffusion and of the optimisation time on optimal unstable structures. Technical Report 192, E.C.M.W.F., Shinfield Park, Reading (U.K.). ECMWF Tech. Memo.

Buizza, R., 1994: Sensitivity of optimal unstable structures. *Quart. J. Roy. Meteor. Soc.*, **120**, 429–451.

Buizza, R., and T.N. Palmer, 1995: The singular vector structure of the atmospheric general circulation. *J. Atmos. Sci.*, **9**, 1434–1456.

Chou, C., and J.D. Neelin, 1996: Linearization of a longwave radiation scheme for intermediate tropical atmospheric model. *J. Geophys. Res.*, . (to appear).

Courtier, P., C. Freydier, J.-F. Geleyn, F. Rabier, and M. Rochas, 1991: The ARPEGE project at METEO-FRANCE. In *ECMWF Seminar on Numerical methods in atmospheric models*, pages 193–232, Shinfield Park, Reading (UK). ECMWF. 9-13 September 1991.

Courtier, P., J.-N. Thépaut, and A. Hollingsworth, 1994: A strategy for operational implementation of 4D-Var using an incremental approach. *Quart. J. Roy. Meteor. Soc.*, **120**, 1367–1387.

Ehrendorfer, M., J.J. Tribbia, and R.M. Errico, 1996: Mesoscale predictability: an assessment through adjoint methods. In *ECMWF Seminar on Predictability*, pages 157–183, Shinfield Park, Reading (UK). ECMWF. 4-8 September 1995.

Errico, R.M., 1997: Diagnostic evaluation of the linearization of physical processes. In *ECMWF Workshop on non-linear aspects of data assimilation*, Shinfield Park, Reading (UK). ECMWF. 9-11 September 1996.

Ferraro, R.R., F. Weng, N.C. Grody, and A. Basist, 1996: An eight-year (1987-1994) time series of rainfall, clouds, water vapor, snow cover and sea-ice derived from SSM/I measurements. *Bull. Amer. Meteor. Soc.*, **77**, 891–905.

Filiberti, M.A., F. Rabier, J.-N. Thépaut, L. Eymard, and P. Courtier, 1997: Four-dimensional variational assimilation of SSM/I water vapour data. *Quart. J. Roy. Meteor. Soc.*, . (submitted).

Fillion, L., and R. Errico, 1997: Variational assimilation of precipitation data using moist-convective parameterization schemes: A 1DVAR study. *Mon. Weather Rev.*, . (submitted).

Gregory, D., and M.J. Miller, 1989: A numerical study of the parametrization of deep tropical convection. *Quart. J. Roy. Meteor. Soc.*, **115**, 1209–1242.

Heckley, W.A., A.G. Kelly, and M. Tiedtke, 1990: On the use of satellite-derived heating rates for data assimilation within the tropics. *Mon. Weather Rev.*, **118**, 1743–1757.

Kasahara, A., J.-I. Tsutsui, and H. Hirakuchi, 1996: Inversion methods of three cumulus parameterizations for diabatic initialization of a tropical cyclone model. *Mon. Weather Rev.*, **124**, 2304–2321.

Krishnamurti, T.N., K. Ingles, S. Cocke, R. Pash, and T. Kitade, 1984: Details of low latitude medium-range numerical weather prediction using a global spectral model. Part II: Effects of orography and physical initialization. *J. Meteor. Soc. Japan*, **62**, 613–649.

Langland, R.H., R.L. Elsberry, and R.M. Errico, 1996: Adjoint sensitivity of an idealized extratropical cyclone with moist physical processes. *Quart. J. Roy. Meteor. Soc.*, **122**, 1891–1920.

Lott, F., and M. Miller, 1995: A new sub-grid orographic drag parametrization: its formulation and testing. Technical Report 218, E.C.M.W.F., Shinfield Park, Reading (U.K.). ECMWF Tech. Memo.

Louis, J.-F., M. Tiedtke, and J.-F. Geleyn, 1982: A short history of the operational PBL parametrization at ECMWF. In *ECMWF Workshop on boundary layer parametrization*, pages 59–79, Shinfield Park, Reading (UK). ECMWF. November 1981.

Molteni, F., R. Buizza, T.N. Palmer, and T. Petroliagis, 1996: The ECMWF Ensemble Prediction System : methodology and validation. *Quart. J. Roy. Meteor. Soc.*, **122**, 73–119.

Phalippou, L., 1996: Variational retrieval of humidity profile, wind speed and cloud liquid-water path with the SSM/I: Potential for numerical weather prediction. *Quart. J. Roy. Meteor. Soc.*, **122**, 327–355.

Puri, K., and M.J. Miller, 1990: The use of satellite data in the specification of convective heating for diabatic initialization and moisture adjustment in numerical weather prediction. *Mon. Weather Rev.*, **118**, 67–93.

Rabier, F., P. Courtier, J. Pailleux, O. Talagrand, J.-N. Thépaut, and D. Vasiljevic, 1993: Comparison of four-dimensional variational assimilation with simplified sequential assimilation. In *ECMWF Workshop on Variational assimilation, with special emphasis on three-dimensional aspects*, pages 271–325, Shinfield Park, Reading (UK). ECMWF. 9-12 November 1992.

Rabier, F., E. Klinker, P. Courtier, and A. Hollingsworth, 1996: Sensitivity of forecast errors to initial conditions. *Quart. J. Roy. Meteor. Soc.*, **122**, 121–150.

Rabier, F., J.-N. Thépaut, and P. Courtier, 1997: Four dimensional variational assimilation at ECMWF. In *ECMWF Seminar on Data Assimilation*, Shinfield Park, Reading (UK). ECMWF. 2-6 September 1996.

Simpson, J., C. Kummerov, W.-K. Tao, and R.F. Adler, 1996: On the Tropical Rainfall Measuring Mission (TRMM). *Meteor. and Atmos. Phys.*, **60**, 19–36.

Slingo, J.M., 1987: The development and verifications of a cloud prediction scheme of the ECMWF model. *Quart. J. Roy. Meteor. Soc.*, **113**, 899–927.

Talagrand, O., and P. Courtier, 1987: Variational assimilation of meteorological observations with the adjoint vorticity equation, I, theory. *Quart. J. Roy. Meteor. Soc.*, **113**, 1311–1328.

Thorpe, A.J., and K.A. Emanuel, 1985: Frontogenesis in the presence of small stability to slantwise convection. *J. Atmos. Sci.*, **42**, 1809–1824.

Tiedtke, M., 1989: A comprehensive mass-flux scheme for cumulus parameterization in large-scale models. *Mon. Weather Rev.*, **117**, 1779–1800.

Tiedtke, M., 1993: Representation of clouds in large-scale models. *Mon. Weather Rev.*, **121**, 3040–3061.

Tsuyuki, T., 1996: Variational data assimilation in the tropics using precipitation data. Part II: 3D Model. *Mon. Weather Rev.*, **124**, 2545–2561.

Verlinde, J., and W.R. Cotton, 1993: Fitting microphysical observations of nonsteady convective clouds to a numerical model: An application of the adjoint technique of data assimilation to a kinematic model. *Mon. Weather Rev.*, **121**, 2776–2793.

Yanai, M., S. Esbensen, and J. Chu, 1973: Determination of bulk properties of tropical clusters from large-scale heat and moisture budgets. *J. Atmos. Sci.*, **30**, 611–627.

Zou, X., I.M. Navon, and J.G. Sela, 1993: Variational data assimilation with moist threshold processes using the NMC spectral model. *Tellus*, **45A**, 370–387.

Zupanski, D., 1993: The effects of discontinuities in the Betts-Miller cumulus convection scheme on four-dimensional variational data assimilation. *Tellus*, **45A**.

Zupanski, D., and F. Mesinger, 1995: Four-dimensional variational assimilation of precipitation data. *Mon. Weather Rev.*, **123**, 1112–1127.